1436 *Inorg. Chem.* **1992**, *31*, 1436–1451

Contribution from the Departments of Chemistry, The Johns Hopkins University, Baltimore, Maryland 21218,
and State University of New York (SUNY) at Albany, Albany, New York 12222

Dioxygen–Copper Reactivity and Functional Modeling of Hemocyanins. Reversible Binding of O_2 and CO to Dicopper(I) Complexes $[Cu^I_2(L)]^{2+}$ (L = Dinucleating Ligand) and the Structure of a Bis(carbonyl) Adduct, $[Cu^I_2(L)(CO)_2]^{2+}$

Kenneth D. Karlin,*[†] Zoltán Tyeklár, Amjad Farooq, Michael S. Haka, Phalguni Ghosh,
Richard W. Cruse, Yilma Gultneh, Jon C. Hayes, Paul J. Toscano,[‡] and Jon Zubieta[§]

Received November 27, 1990

The reversible binding of CO and O_2 to dinuclear copper(I) complexes is described in chemical systems which mimic to a significant extent a number of properties of the copper-containing dioxygen carrier protein hemocyanin (Hc). Various dicopper(I) complexes have been synthesized; these utilize neutral dinucleating ligands L, in which two tridentate PY2 units (PY2 = bis[2-(2-pyridyl)ethyl]amine) are connected by a variable alkyl chain $-(CH_2)_n-$ (L = N*n*, *n* = 3–5). These include $[Cu_2(L)]^{2+}$ (**1**, L = N*n*, *n* = 3–5), which are tricoordinate dicopper(I) complexes, and $[Cu_2(L)(L')_2]^{2+}$ (**3**, L = N*n* and L′ = CH_3CN; **4**, L′ = CO; **5**, L′ = PPh_3), which are bisadducts possessing tetracoordinate Cu(I) moieties. All of these dicationic compounds are isolated as either perchlorate or hexafluorophosphate salts. The binding of CO to **1** is reversible, as indicated by the ability to regenerate **1** by the application of a vacuum to dichloromethane solutions of $[Cu_2(Nn)(CO)_2]^{2+}$ (**4**) at room temperature. The structure of the bis(carbonyl) adduct $[Cu_2(N3)(CO)_2](ClO_4)_2$ (**4a**$(ClO_4)_2$) has been determined by X-ray crystallographic studies, and the results are described. Complex **4a**$(ClO_4)_2$ crystallizes in monoclinic space group $P2_1/n$ with $a = 10.255$ (2) Å, $b = 25.943$ (3) Å, $c = 14.767$ (3) Å, $\beta = 94.94$ (1)°, and $Z = 4$ and was refined to $R = 0.0781$. Both complexes **1** and **3** serve as precursors to the dioxygen adducts $[Cu_2(Nn)(O_2)]^{2+}$ (**2**), which form and are stable only at low temperatures, i.e., −80 °C, in dichloromethane solutions. These species are characterized by strong and multiple electronic neutral absorptions in the visible region, including a prominent band in the 350–360-nm range (ϵ = 14000–21400 M^{-1} cm^{-1}). The reaction of **1** with O_2 is reversible, and the application of a vacuum to the dioxygen adduct (**2**) formed removes the bound O_2 and regenerates **1**. The recovered dioxygen can be identified both qualitatively and quantitatively (a gravimetric method is described), and the *vacuum cycling* can be followed spectrophotometrically over several cycles. In addition, saturating a −80 °C solution of the dioxygen complexes with carbon monoxide results in the displacement of the O_2 ligand with the resulting formation of the bis(carbonyl) adducts $[Cu_2(Nn)(CO)_2]^{2+}$ (**4**). *Carbonyl cycling*, where **1** reacts with O_2 to produce **2**, dioxygen is displaced by CO to give **4**, and **4** is decarbonylated to regenerate **1**, can also be followed spectrophotometrically over several cycles. Manometric measurements indicate that the stoichiometry of the reaction of **1** or **3** with O_2 at −80 °C is Cu:O_2 = 2:1, and a variety of other evidence (e.g. X-ray absorption spectroscopy, UV–vis CT bands, presence of d–d bands) lead to the conclusion that complexes $[Cu_2(Nn)(O_2)]^{2+}$ (**2**) are best described as peroxodicopper(II) complexes, formed by reactions of O_2 with **1** in an intramolecular process. Other characteristics of these $\{Cu_2-O_2\}^{2+}$ species are described, including EPR (silent), ^1H NMR (normal), and magnetic behavior (essentially diamagnetic). The electrochemical properties (cyclic voltammetry) of **1** and **2** are also reported. A novel bent μ-η^2:η^2-peroxo–dicopper(II) structure is proposed for $[Cu_2(L)(O_2)]^{2+}$ (**2**), consistent with the physical properties observed as in line with the recent important structure described by Kitajima and co-workers (*J. Am. Chem. Soc.* **1992**, *114*, 1277–1291). Comparison of $[Cu_2(Nn)(O_2)]^{2+}$ (**2**) with other types of $\{Cu_2-O_2\}$ complexes are made, including when L is a *m*-xylyl group (L = XYL-X), where complexes like **2** are seen to be intermediates in the hydroxylation reactions which occur when $[Cu_2(XYL-H)]^{2+}$ (**1e**) is reacted with O_2. The biological relevance of the studies is discussed, and a structure similar to that occurring in $[Cu_2(L)(O_2)]^{2+}$ (**2**) is suggested to occur in oxyhemocyanin.

Introduction

We have recently described several classes of peroxodicopper(II) complexes, which are formed reversibly from the reaction of Cu(I) precursors with dioxygen (O_2).[1] One of these consists of dicationic dinuclear complexes $[Cu_2(L)(O_2)]^{2+}$ (**2**), where L is a dinucleating ligand containing hydrocarbon linkers which connect two tridentate donor bis[2-(2-pyridyl)ethyl]amine (PY2) units, e.g. N3, N3OR, N4, N5, or XYL-X (Figure 1).[2,3] Thus, the hydrocarbon linker group can consist of a methylene chain of variable length ($-(CH_2)_n-$, *n* = 3–5)[1,2] or a *m*-xylyl group.[1,4,5] At −80 °C in dichloromethane, tricoordinate dicopper(I) complexes $[Cu_2(L)]^{2+}$ (**1a–d**) or tetracoordinate species $[Cu_2(Nn)(L')_2]^{2+}$ (**3**, L′ = CH_3CN) react reversibly with O_2 to give complexes formulated as $[Cu_2(Nn)(O_2)]^{2+}$ (**2a–d**), since manometric O_2-uptake measurements indicate that Cu:O_2 = 2:1. The application of a vacuum to the dioxygen adducts formed removes the bound O_2 and regenerates the dicopper(I) complex **1**. Saturating the solutions of dioxygen complexes (**2**) with CO causes displacement of the O_2 ligand with the formation of the bis(carbonyl)dicopper(I) complexes $[Cu_2(Nn)(CO)_2]^{2+}$ (**4**), and the latter can also be generated directly from **1** upon addition of carbon monoxide at room temperature. The CO substitution reaction undoubtedly occurs by forcing the dioxygen binding equilibrium toward the deoxygenated form (**1**), with subsequent reaction with CO (Figure 1).

There are a number of features of this class of dioxygen adducts $[Cu_2(L)(O_2)]^{2+}$ (**2**) which make them particularly interesting. First, they serve as potential structural, functional, and spectro-

---

[†] To whom correspondence should be addressed at the Department of Chemistry, The Johns Hopkins University, Charles & 34th Streets, Baltimore, MD 21218.

[‡] SUNY at Albany.

[§] Current address: Department of Chemistry, Syracuse University, Syracuse, NY 13244.

(1) (a) Tyeklár, Z.; Karlin, K. D. *Acc. Chem. Res.* **1989**, *22*, 241–248 and references cited therein. (b) Tyeklár, Z.; Ghosh, P.; Karlin, K. D.; Farooq, A.; Cohen, B. I.; Cruse, R. W.; Gultneh, Y.; Haka, M. S.; Jacobson, R. R.; Zubieta, J. In *Metal Clusters in Proteins*; Que, L., Jr., Ed., ACS Symposium Series No. 372; American Chemical Society: Washington, DC, 1988; Chapter 5, pp 85–104. (c) Sanyal, I.; Strange, R. W.; Blackburn, N. J.; Karlin, K. D. *J. Am. Chem. Soc.* **1991**, *113*, 4692–4693.

(2) (a) Karlin, K. D.; Haka, M. S.; Cruse, R. W.; Meyer, G. J.; Farooq, A.; Gultneh, Y.; Hayes, J. C.; Zubieta, J. *J. Am. Chem. Soc.* **1988**, *110*, 1196–1207. (b) Blackburn, N. J.; Strange, R. W.; Farooq, A.; Haka, M. S.; Karlin, K. D. *J. Am. Chem. Soc.* **1988**, *110*, 4263–4272. (c) Karlin, K. D.; Haka, M. S.; Cruse, R. W.; Gultneh, Y. *J. Am. Chem. Soc.* **1985**, *107*, 5828–5829. (d) Blackburn, N. J.; Strange, R. W.; Reedijk, J.; Volbeda, A.; Farooq, A.; Karlin, K. D.; Zubieta, J. *Inorg. Chem.* **1989**, *28*, 1349–1357 and references cited therein.

(3) In previous publications,[1b,2a–c] this class of ligands has been referred to as N*n*PY2.

(4) (a) Karlin, K. D.; Gultneh, Y.; Hayes, J. C.; Cruse, R. W.; McKown, J.; Hutchinson, J. P.; Zubieta, J. *J. Am. Chem. Soc.* **1984**, *106*, 2121–2128. (b) Karlin, K. D.; Gultneh, Y.; Hutchinson, J. P.; Zubieta, J. *J. Am. Chem. Soc.* **1982**, *104*, 5240–5242.

(5) Karlin, K. D.; Cruse, R. W.; Haka, M. S.; Gultneh, Y.; Cohen, B. I. *Inorg. Chim. Acta* **1986**, *125*, L43–L44.

0020-1669/92/1331-1436$03.00/0

scopic model systems for hemocyanins (Hc's),[6,7] the arthropodan and molluscan dioxygen-transporting proteins, in which a dinuclear dicopper ion site interacts with dioxygen. Aside from their reversible O_2-binding capability, species **2** are also characterized by multiple and strong charge-transfer absorption bands in the visible region, spectral patterns which are unique in copper/dioxygen coordination chemistry and which also qualitatively resemble those observed for hemocyanins.[1,2a] In addition, complexes $[Cu_2(Nn)(O_2)]^{2+}$ (**2**) (L = N*n* = $-(CH_2)_n-$ linked dinucleating ligand) serve to replicate the $\{Cu_2-O_2\}^{2+}$ species which we have previously shown to be an intermediate in a model monooxygenase system we have described earlier.[1,4] There, in a process reminiscent of the reaction that occurs in tyrosinase (Tyr),[8] $[Cu^I_2(XYL\text{-}H)]^{2+}$ (**1e**, XYL-H is a *m*-xylyl group linked by two PY2 units; Figure 1) cleanly reacts with O_2 leading to the hydroxylation of the xylene group and forming the phenoxo- and hydroxo-bridged dicopper(II) complex $[Cu^{II}_2(XYL\text{-}O\text{-})(OH)]^{2+}$.[4] Recent kinetic studies[9] and other chemical information demonstrate that there is an initial reversible reaction of O_2 with **1e** to give a species analogous to **2a–d**, i.e. $[Cu^I_2(XYL\text{-}H)(O_2)]^{2+}$ (**2e**), which is followed by an irreversible attack by the coordinated O_2 moiety on the arene substrate to produce $[Cu^{II}_2(XYL\text{-}O\text{-})(OH)]^{2+}$.[1,10]

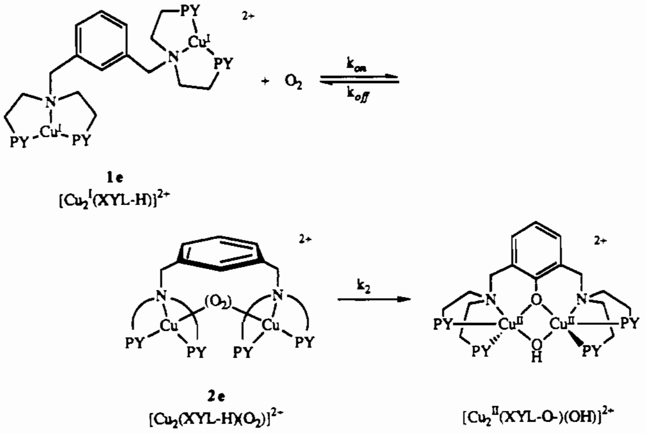

1e

$[Cu_2^I(XYL\text{-}H)]^{2+}$

2e

$[Cu_2(XYL\text{-}H)(O_2)]^{2+}$

$[Cu_2^{II}(XYL\text{-}O\text{-})(OH)]^{2+}$

We have previously described the reversible binding CO and O_2 chemistry of the complex $[Cu_2(N4)]^{2+}$, where N4 is the ligand with a $-(CH_2)_4-$ chain linking the PY2 units;[2a] this report included the structural characterizations of two precursor dicopper(I) complexes, $[Cu_2(N4)](ClO_4)_2$ (with Cu^I–PY2 coordination and weaker perchlorate interactions) and $[Cu_2(N4)(CH_3CN)_2]^{2+}$. Here, we report the particulars of the chemistry associated with dinucleating ligands containing either a three (N3, N3OR) or five (N5) carbon methylene chain linker group (Figure 1). In addition to synthetic and spectroscopic details associated with the CO- and O_2-binding chemistry, we report the electrochemical characterization of $[Cu_2(Nn)]^{2+}$ (**1a–c**) and $[Cu_2(Nn)(O_2)]^{2+}$ (**2a–c**) and the full X-ray structural description of the bis(carbonyl) adduct $[Cu_2(N3)(CO)_2]^{2+}$ (**4a**). We compare and contrast the properties of all of these complexes as a function of the dinucleating ligand hydrocarbon linker group, and we summarize the properties and probable structures of this class of $Cu_2–O_2$ complexes and their biological relevance.

Experimental Section

Materials and Methods. The general preparative procedures and methods for characterization of complexes have been previously described.[2a,11]

Synthesis of Ligands and Complexes. N3 and N5. The α,ω-diaminoalkane (1,3-diaminopropane for N3 and 1,5-diaminopentane for N5) (0.1 mol) was added to a solution of 2-vinylpyridine (105.1 g, 1 mol) and acetic acid (30.0 g, 0.5 mol) in 150 mL of methanol. The mixture was refluxed for 10 days. The methanol was removed by rotary evaporation, and the resulting brown oil was taken up in dichloromethane (300 mL) and then washed with 10% sodium hydroxide solution (3 × 100 mL). The organic layer was dried over anhydrous magnesium sulfate, and then the solvent was pumped off. Excess 2-vinylpyridine was distilled off in high vacuum leaving 50–55 g of the crude product. It was added to 300 mL of benzene in which phthalic anhydride (5.0 g, e.g. 10% by weight) was dissolved and stirred. After 1 h, the mixture was monitored by TLC (silica gel, 98% methanol–2% ammonium hydroxide as eluant). If more than one spot was observed, additional phthalic anhydride (1 g) was added and the mixture stirred for an additional 1 h. When only one spot was observed, the mixture was extracted with 10% sodium hydroxide solution (3 × 100 mL). The organic phase was dried over magnesium sulfate and then passed through a short column containing ca. 50 g of silica gel. The solvent was pumped off on rotary evaporator to give the pure, orange ligand (yield: 35–40 g, 70–80% based on the diamine). Data for N3 are as follows. TLC (98% CH_3OH–2% NH_4OH): R_f 0.77. ^1H NMR ($CDCl_3$): δ 1.3–1.75 (2 H, m br), 2.20–2.65 (4 H, br t), 2.91 (16 H, s), 6.70–7.00 (8 H, py-3, py-5, br m), 7.05–7.50 (4 H, py-4, br m), 8.15–8.40 (4 H, py-6, br d). ^{13}C NMR (77.0 MHz, $CDCl_3$): δ 24.73 (CH_2), 35.71 (py–CH_2), 51.86 (CH_2–N–CH_2), 53.77 (CH_2), 120.96 (py C-5), 123.32 (py C-3), 136.12 (py C-4), 149.08 (py C-6), 160.56 (py C-2). Data for N5 are as follows. TLC (98% CH_3OH–2% NH_4OH): R_f 0.76. ^1H NMR ($CDCl_3$): δ 1.05–1.55 (6 H, br m), 2.25–2.65 (4 H, br m), 2.90 (16 H, s), 6.80–7.10 (8 H, py-3, py-5, br m), 7.25–7.60 (4 H, py-4, br m), 8.30–8.50 (4 H, py-6, br d). ^{13}C NMR ($CDCl_3$): δ 25.22 (CH_2), 27.10 (CH_2), 35.88 (CH_2), 53.80 (CH_2), 53.80 (CH_2), 120.83 (py C-5), 123.20 (py C-3), 135.91 (py C-4), 148.95 (py C-6), 160.64 (py C-2).

N3OH. An excess of 2-vinylpyridine (95.7 g, 0.91 mmol, purified by passing it through a short silica gel precolumn using diethyl ether solvent, followed by removal of the ether by rotary evaporation) was added to a solution of 1,3-diamino-2-hydroxypropane (8.22 g, 91.0 mmol) in methanol (200 mL). Acetic acid (27.4 g, 46 mmol) was used as a catalyst. The reactants were stirred while being heated near reflux for 7 days. The MeOH was removed by rotary evaporation, and the resulting oil was washed with 140 mL of 15% aqueous NaOH and extracted with dichloromethane (3 × 75 mL). The dichloromethane solution was washed with water (3 × 75 mL), dried over anhydrous $MgSO_4$, and filtered. The solvent was removed by rotary evaporation. The resulting oil was placed in vacuo at 40 °C overnight to remove the excess 2-vinylpyridine. A total of 46.0 g of the crude product was obtained. Typically, 9.0 g was chromatographed through a column of alumina (80–200 mesh, MCB) by using ethyl acetate–methanol (9:1, v/v) as eluant (R_f 0.64) to give 6.6 g of the pure product (73% yield based on the diamine). ^1H NMR ($CDCl_3$): δ 2.4 (4 H, d), 2.8 (16 H, br s), 3.5 (1 H, br s), 3.75 (1 H, br s), 6.7–7.0 (8 H, m), 7.1–7.4 (4 H, m), 8.2 (4 H(py-6), br d). ^{13}C NMR (57.3 MHz, CD_2Cl_2): δ 36.42 (CH_2–C–CH_2), 59.59 (py–CH_2–CH_2), 67.18 (CH_2–*C*–CH_2), 121.38 (py C-5), 123.72 (py C-3), 136.39 (py C-4), 149.53 (py C-6), 161.26 (py C-2). ^1H NMR (CD_2Cl_2): δ 2.35 (4 H, br s), 2.77 (16 H, br m), 3.48 (1 H, br s), 4.0 (1 H, br s), 6.96 (8 H, br s), 7.43 (4 H, br m), 8.35 (4 H(py-6), br s).

N3OR. To a solution of N3OH (4.00 g, 7.84 mmol) in 50 mL of dry THF, containing triethylamine (2.38 g, 23.5 mmol), was added dropwise a solution of 4-biphenylcarbonyl chloride (0.26 g, 1.20 mmol) in 50 mL of dry THF. The reactants were stirred under argon for 1 day, while the solution was allowed to warm up slowly to room temperature. The reaction mixture was filtered through a medium-porosity filter paper, and the white precipitate was washed with 30 mL of dry THF. The washings were combined with the filtrate. The THF was removed by rotary evaporation. The resulting yellow oil (4.29 g) was chromatographed on alumina with a mixture of ethyl acetate and methanol (40:1, v/v) solvent system (R_f 0.49) to give 3.40 g of the pure product (63% yield based on N3OH). ^1H NMR ($CDCl_3$): δ 2.82 (20 H, m), 3.80 (1 H, s), 6.5–8.0

---

(6) (a) Solomon, E. I. In *Metal Clusters in Proteins*; Que, L., Jr., Ed.; ACS Symposium Series 372; American Chemical Society: Washington, DC, 1988; pp 116–150. (b) Solomon, E. I. In *Metal Ions in Biology*; Spiro, T. G., Ed.; Wiley-Interscience: New York, 1981; Vol. 3, pp 41–108. (c) Solomon, E. I.; Penfield, K. W.; Wilcox, D. E. *Struct. Bonding (Berlin)* **1983**, *53*, 1–57. (d) Lontie, R.; Witters, R. *Met. Ions Biol. Syst.* **1981**, *13*, 229–258.

(7) Volbeda, A.; Hol, W. G. J. *J. Mol. Biol.* **1989**, *209*, 249–279.

(8) (a) Wilcox, D. E.; Porras, A. G.; Hwang, Y. T.; Lerch, K.; Winkler, M. E.; Solomon, E. I. *J. Am. Chem. Soc.* **1985**, *107*, 4015–4027. (b) Robb, D. A. In *Copper Proteins and Copper Enzymes*; Lontie, R., Ed.; CRC: Boca Raton, FL, 1984; Vol. 2, pp 207–241. (c) Lerch, K. *Met. Ions Biol. Syst.* **1981**, *13*, 143–186.

(9) Cruse, R. W.; Kaderli, S.; Karlin, K. D.; Zuberbühler, A. D. *J. Am. Chem. Soc.* **1988**, *110*, 6882–6883.

(10) (a) Karlin, K. D.; Cohen, B. I.; Jacobson, R. R.; Zubieta, J. *J. Am. Chem. Soc.* **1987**, *109*, 6194–6196. (b) Nasir, M. S.; Cohen, B. I.; Karlin, R. D. *J. Am. Chem. Soc.* **1992**, *114*, 2482–2494.

(11) (a) Jacobson, R. R.; Tyeklár, Z.; Farooq; Karlin, K. D.; Liu, S.; Zubieta, J. *J. Am. Chem. Soc.* **1988**, *110*, 3690–3692. (b) Karlin, K. D.; Cruse, R. W.; Gultneh, Y.; Farooq, A.; Hayes, J. C.; Zubieta, J. *J. Am. Chem. Soc.* **1987**, *109*, 2668–2679.

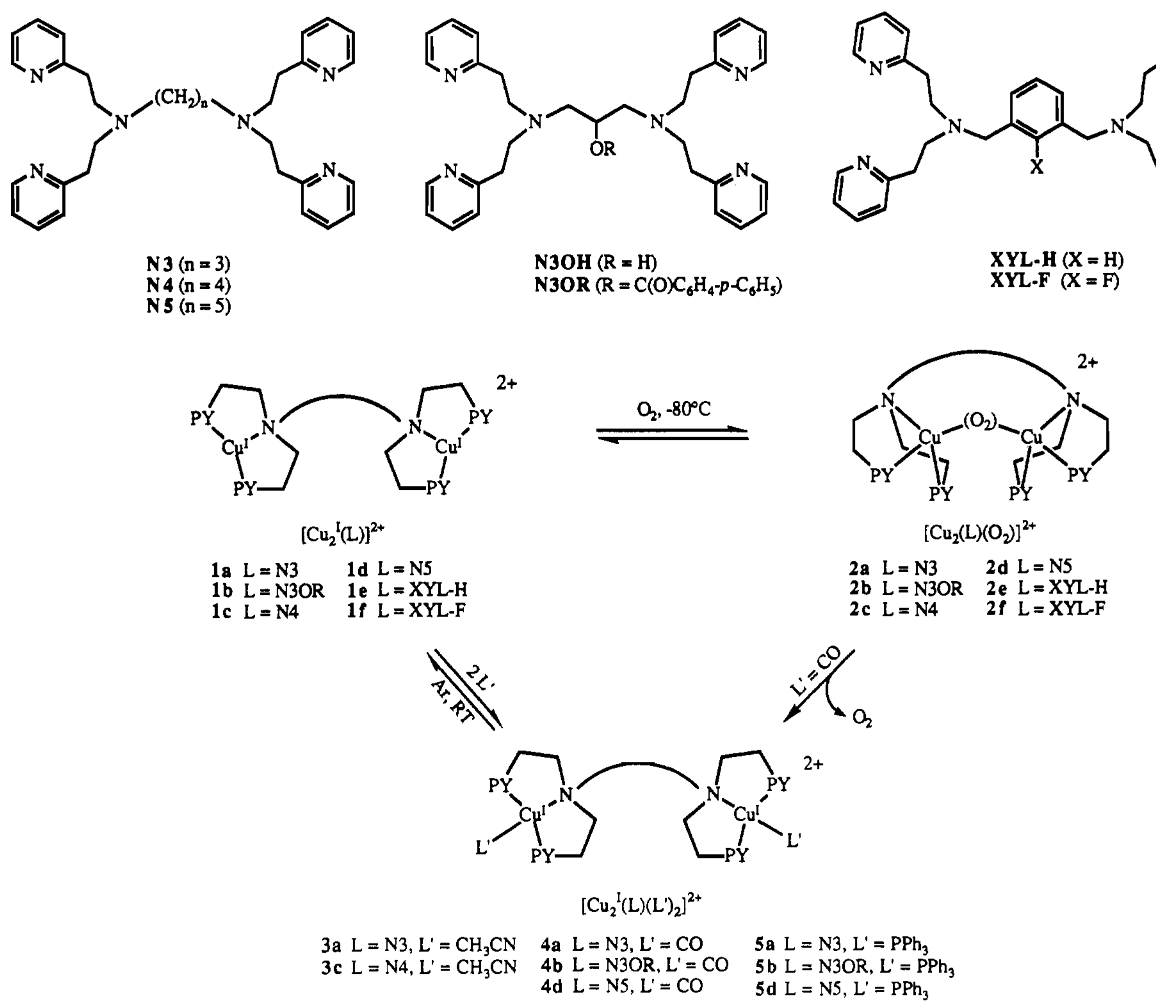

Figure 1. Scheme showing the dinucleating N*n* and XYL-X ligands and the reactions of the dicationic dicopper(I) species. Tricoordinate-containing compounds $[Cu_2(L)]^{2+}$ (**1**) form bis(adduct) complexes $[Cu_2(L)(L')_2]^{2+}$ (**3**, L′ = CH_3CN; **4**, L′ = CO; **5**, L′ = PPh_3). The binding of CO is reversible, such that bubbling carbon monoxide through solutions of **1** readily gives **4**, while the latter can be decarbonylated through vacuum/purge cycles. $[Cu_2(L)]^{2+}$ (**1**) react reversibly with O_2 at −80 °C in dichloromethane to give the dioxygen adducts $[Cu_2(L)(O_2)]^{2+}$ (**2**), which are best described as peroxodicopper(II) complexes. Carbon monoxide also reacts with **2** to give the bisadduct **4**, displacing O_2 in the process. See the text for further discussion.

(21 H, py-3, py-4, py-5, Ph–Ph–, m), 8.17 (4 H, py-6, br d). ^{13}C NMR (57.3 MHz, CD_2Cl_2): δ 36.45 (CH_2–C–CH_2), 56.40 (py–CH_2–CH_2), 72.60 (CH_2–C–CH_2), 121.36 (py C-5), 123.68 (py C-3), 136.33 (py C-4), 149.58 (py C-6), 161.18 (py C-2), 166.13 (OCO), 127.40, 127.63, 128.60, 129.42, 130.13, 130.64, 140.39, 145.67 (biphenyl group); the CO resonance was not observed.

$[Cu_2(N3)](ClO_4)_2$ (1a$(ClO_4)_2$). A solution of N3 (0.50 g, 1.01 mmol) in 40 mL of CH_2Cl_2 was added dropwise, with stirring, to solid $[Cu(CH_3CN)_4]ClO_4$[12] (0.66 g, 2.02 mmol) under argon. The resulting clear yellow solution was allowed to stir for 2 h. Precipitation by addition of diethyl ether afforded 0.69 g of a bright yellow microcrystalline powder (83% yield). Repeated recrystallization diminished the amount of strongly coordinated CH_3CN, and this was monitored using ^1H NMR spectroscopy. Three to four such recrystallization using CH_2Cl_2–Et_2O (1:2, v/v) produced 0.54 g (65%) of a bright yellow microcrystalline material. Anal. Calcd for $C_{31}H_{38}Cl_2Cu_2N_6O_8$: C, 45.37; H, 4.67; N, 10.24. Found: C, 44.73; H, 4.60; N, 10.10. ^1H NMR (CD_3NO_2): δ 1.00–1.60 (2 H, br m), 2.00–2.55 (4 H, br m), 3.00 (16 H, s), 7.10–7.50 (8 H, py-3, py-5, br m), 7.5–8.00 (4 H, py-4, br m), 8.35–8.70 (4 H, py-6, br d). ^{13}C NMR (57.3 MHz, CD_3NO_2): δ 19.30 (CH_2), 29.34 (CH_2), 49.79 (CH_2), 54.98 (CH_2), 118.97 (py C-5), 121.12 (py C-3), 135.19 (py C-4), 146.11 (py C-6), 157.04 (py C-2). IR (Nujol): 1600 (C=C, s), 1560 (C=C, s), 1050 (ClO_4^-, s, br) cm^{-1}.

$[Cu_2(N3OR)](PF_6)_2 \cdot CH_2Cl_2$ (1b$(PF_6)_2 \cdot CH_2Cl_2$). A 250-mL Schlenk flask was charged with $[Cu(CH_3CN)_4]PF_6$[13] (0.90 g, 2.42 mmol) in the air. A 250-mL addition funnel was attached to the flask. The whole system was evacuated and purged with argon three times, and a solution of the ligand N3OR (0.90 g, 1.30 mmol) in 30 mL of dry CH_3OH was then transferred to the addition funnel under argon. This solution was bubbled with argon for 20 min and added with stirring to the solid $[Cu(CH_3CN)_4]PF_6$. After 2–3 min a yellow solution was formed which then converted slowly to a yellow suspension over a period of ca. 25 min. Diethyl ether (250 mL) was put into the addition funnel and bubbled with Ar for 20 min and added with stirring to the yellow mixture to precipitate out more product. The addition funnel was removed, the flask was stoppered, and the mixture was kept at room temperature overnight. The solvent was decanted, and the precipitate was washed with 100 mL of air-free Et_2O and dried in vacuo giving crude **1b**$(PF_6)_2$. This was redissolved in 50 mL of dichloromethane, and the mixture was filtered under argon. Diethyl ether (200 mL) was layered on the filtrate. Needle-shaped yellow crystals formed from the yellow solution at room temperature in 1 day. The ether layer was decanted under Ar, and the crystals of $[Cu_2(N3OR)](PF_6)_2 \cdot CH_2Cl_2$ (**1b**$(PF_6)_2 \cdot CH_2Cl_2$) (1.30 g, 90%) were washed with diethyl ether and dried under vacuum. Anal. Calcd for $C_{45}H_{48}Cl_2Cu_2F_{12}N_6O_2P_2$: C, 45.30; H, 4.03; N, 7.05. Found: C, 45.98; H, 4.06; N, 7.17. ^1H NMR ($(CD_3)_2CO$): δ 2.4–3.4 (20 H, m), 3.90 (1 H, br s), 5.28 (2 H, CH_2Cl_2), 6.8–7.9 (21 H, py-3, py-4, py-5, Ph–Ph–, m), 8.15 (4 H, py-6, br d). ^{13}C NMR (57.3 MHz, CD_2Cl_2): δ 34.50 (CH_2–C–CH_2), 58.25 (py–CH_2–CH_2), 72.23 (CH_2–C–CH_2), 123.72 (py C-5), 126.29 (py C-3), 139.50 (py C-4), 150.95 (py C-6), 160.47 (py C-2), 166.76 (OCO), 127.30, 127.51, 127.64, 129.06, 129.46, 130.68, 139.70, 147.31 (biphenyl group). IR (Nujol): 1680 (C=O, s), 833 (PF_6^-, s, br) cm^{-1}.

$[Cu_2(N3)(CH_3CN)_2](ClO_4)_2$ (3a$(ClO_4)_2$). N3 (0.50 g, 1.01 mmol), dissolved in 20 mL of CH_3CN, was added dropwise, with stirring under argon, to solid $[Cu(CH_3CN)_4]ClO_4$[12] (0.66 g, 2.02 mmol). The resulting clear golden solution was then allowed to stir for 2 h. Precipitation with diethyl ether afforded a dark yellow-brown microcrystalline material

---

(12) Hemmerich, P.; Sigwart, C. *Experimentia* **1963**, *19*, 488.
(13) Kubas, G. J. *Inorg. Synth.* **1979**, *19*, 90.

which was isolated by filtration under argon. Recrystallization with CH_3CN-Et_2O (1:4, v/v) produced a microcrystalline material, 0.69 g (76% yield). Anal. Calcd for $C_{35}H_{44}Cl_2Cu_2N_8O_8$: C, 46.56; H, 4.91; N, 12.41. Found: C, 46.01; H, 4.86; N, 11.47. ^1H NMR (CD_3NO_2): δ 1.50–2.00 (2 H, br m), 2.10–2.30 (6 H, CH_3CN, m), 2.40–3.20 (20 H, br m), 7.00–7.45 (8 H, py-3, py-5, br m), 7.50–7.90 (4 H, py-4, br m), 8.25–8.55 (4 H, py-6, br d). ^{13}C NMR (57.3 MHz, CD_3NO_2): δ −3.42 (CH_3CN), 18.71 (CH_2), 30.38 (CH_2), 50.43 (CH_2), 118.90 (py C-5), 121.44 (py C-3), 134.71 (py C-4), 145.89 (py C-6), 156.96 (py C-2). IR (Nujol): 1600 ($C=C$, s), 1560 ($C=C$, s), 1080 (ClO_4^-, br) cm^{-1}.

$[Cu_2(N3)(CO)_2](PF_6)_2$ (4a$(PF_6)_2$). N3 (0.50 g, 1.01 mmol), in 20 mL of carbon monoxide-saturated CH_3OH, was added dropwise, with stirring, to solid $[Cu(CH_3CN)_4]PF_6$[13] (0.75 g, 2.02 mmol). The solid initially dissolved, and within a few minutes a fine faint-yellow precipitate formed. The mixture was allowed to stir for 2 h at which time diethyl ether was added to precipitate out more product. The solution was then filtered under Ar producing 0.85 g of an off-white fine powder (87% yield). The product was then recrystallized from $CH_2Cl_2-Et_2O$ (1:2, v/v) under CO atmosphere providing crystalline material, 0.753 g (77% yield). Anal. Calcd for $C_{33}H_{38}Cu_2F_{12}N_6O_2P_2$: C, 40.96; H, 3.96; N, 8.68. Found: C, 40.77; H, 4.12; N, 8.17. ^1H NMR (CD_3NO_2): δ 1.70–2.25 (2 H, br m), 2.50–3.30 (20 H, br m), 7.05–7.50 (8 H, py-3, py-5, br m), 7.55–7.95 (4 H, py-4, br, m), 8.10–8.50 (4 H, py-6, br d). ^{13}C NMR (57.3 MHz, CD_3NO_2): δ 18.55 (CH_2), 30.55 (CH_2), 50.48 (CH_2), 119.16 (py C-5), 121.57 (py C-3), 135.37 (py C-4), 146.38 (py C-6), 157.00 (py C-2). IR (Nujol): 2080 (CO, s), 1605 ($C=C$, s), 1568 ($C=C$, s), 840 (PF_6^-, s, br) cm^{-1}.

$[Cu_2(N3OR)(CO)_2](PF_6)_2$ (4b$(PF_6)_2$). To solid $[Cu(CH_3CN)_4]PF_6$[13] (0.5 g, 1.34 mmol) was added dropwise, with stirring, a carbon monoxide-saturated solution of the ligand, N3OR (0.48 g, 0.69 mmol), in 50 mL of methanol under argon. The solid dissolved within a few minutes and a yellow solution formed. A 200-mL volume of CO-saturated diethyl ether was layered on the yellow solution resulting in the formation of an off-white microcrystalline material at room temperature in 1 day. This material was first recrystallized from $CH_2Cl_2-Et_2O$ (1:5, v/v) and then from $MeOH-Et_2O$ (1:5, v/v) under CO atmosphere to give 0.50 g (64%) of microcrystalline yellow-white product. Anal. Calcd for $C_{46}H_{46}Cu_2F_{12}N_6O_4P_2$: C, 47.46; H, 3.95; N, 7.22. Found: C, 47.31; H, 4.19; N, 7.95. ^1H NMR (CD_2Cl_2): δ 2.5–3.5 (20 H, m), 5.02 (1 H, br s), 7.1–8.10 (21 H, py-3, py-4, py-5, Ph–Ph–, m), 8.36 (4 H, py-6, br d). ^{13}C NMR (57.3 MHz, CD_2Cl_2): δ 33.56 ($\mathit{C}H_2-C-\mathit{C}H_2$), 57.35 (py–$\mathit{C}H_2-\mathit{C}H_2$), 71.05 ($CH_2-\mathit{C}-CH_2$), 122.72 (py C-5), 125.27 (py C-3), 138.48 (py C-4), 150.05 (py C-6), 159.49 (py C-2), 165.73 (O*C*O), 126.42, 126.52, 126.64, 128.07, 128.48, 129.72, 138.66, 146.28 (biphenyl group); *C*O resonance not observed. ^1H NMR (CD_3NO_2): δ 3.16 (20 H, br s), 6.8–7.95 (21 H, py-3, py-4, py-5, –Ph–Ph, m), 8.28 (4 H, py-6, br d). IR (Nujol): 2073 (CO, s), 1718 ($C=O$, s), 840 (PF_6^-, s, br) cm^{-1}.

$[Cu_2(N5)(CO)_2](PF_6)_2$ (4d$(PF_6)_2$). The synthesis and purification of this complex was analogous to that of $[Cu_2(N3)(CO)_2](PF_6)_2$ (**4a**$(PF_6)_2$). The initial yield was 0.68 g (72%). Upon recrystallization in $CH_2Cl_2-Et_2O$ (1:2, v/v), 0.57 g (60%) of analytically pure pale yellow crystalline material was isolated. Anal. Calcd for $C_{35}H_{42}Cu_2F_{12}N_6O_2P_2$: C, 42.22; H, 4.25; N, 8.44. Found: C, 41.94; H, 4.32; N, 8.35. ^1H NMR (CD_3NO_2): δ 0.90–1.35 (6 H, br m), 2.10–2.30 (4 H, br m), 3.05 (16 H, s), 7.00–7.50 (8 H, py-3, py-5, br m), 7.6–8.00 (4 H, py-4, br m), 8.30–8.60 (4 H, py-6, br d). ^{13}C NMR (57.3 MHz, CD_3NO_2): δ 21.42 ($\mathit{C}H_2$), 29.76 ($\mathit{C}H_2$), 50.14 ($\mathit{C}H_2$), 54.70 ($\mathit{C}H_2$), 119.02 (py C-5), 121.25 (py C-3), 135.31 (py C-4), 146.22 (py C-6), 157.14 (py C-2). IR (Nujol): 2095 (CO, s), 1620 ($C=C$, s), 1582 ($C=C$, s), 840 (PF_6^-, s, br) cm^{-1}.

$[Cu_2(N3)PPh_3)_2](ClO_4)_2$ (5a$(ClO_4)_2$). Compound **4a**$(ClO_4)_2$ (0.78 g, 0.89 mmol) was dissolved in 20 mL of CH_2Cl_2 under argon, producing a light yellow clear solution. A CH_2Cl_2 solution (20 mL) of triphenylphosphine (PPh_3) (0.47 g, 1.78 mmol) was then added, with stirring, to the solution. Effervescence was immediately seen, indicating CO evolution, with the solution now almost colorless. Precipitation with diethyl ether afforded a fine yellow-white precipitate which was collected by filtration under Ar, 1.05 g (88% yield). Recrystallization with $CH_2Cl_2-Et_2O$ (1:2, v/v) afforded a light tan powder which was then washed with a 75-mL portion of diethyl ether to remove the traces of excess triphenylphosphine. This produced an analytically pure product, 1.02 g (86% yield). Anal. Calcd for $C_{67}H_{68}Cl_2Cu_2N_6O_8P_2$: C, 59.82; H, 5.09; N, 6.25. Found: C, 58.90; H, 5.00; N, 6.35. ^1H NMR (CD_2Cl_2): δ 1.70–3.05 (22 H, br m), 6.90–7.85 (42 H, py-3, py-4, py-5, $(P(C_6H_5)_3)_2$, br m), 8.00–8.25 (4 H, py-6, br d). IR (Nujol): 1600 ($C=C$, s), 1570 ($C=C$, s), 1060 (ClO_4^-, br) cm^{-1}.

$[Cu_2(N3OR)(PPh_3)_2](PF_6)_2$ (5b$(PF_6)_2$). A mixture of triphenylphosphine (0.12 g, 0.46 mmol) and **1b**$(PF_6)_2\cdot CH_2Cl_2$ (0.27 g, 0.23 mmol) was dissolved in 20 mL of CH_2Cl_2 under argon, and the mixture was allowed to stir for 30 min. Diethyl ether (150 mL) was layered on the solution. Upon standing overnight at room temperature, an oil deposited out of the solution. The supernatant solution was decanted, and the oil was dried in vacuo and then washed with diethyl ether (100 mL) to give a yellow-white powder which was recrystallized from $MeOH-Et_2O$ (1:5, v/v) and then from $CH_2Cl_2-Et_2O$ giving 0.26 g (70%) of white crystalline solid. Anal. Calcd for $C_{80}H_{76}Cu_2F_{12}N_6O_2P_4$: C, 58.83; H, 4.66; N, 5.15. Found: C, 58.42; H, 4.60; N, 5.49. ^1H NMR (CD_3NO_2): δ 2.5–3.4 (21 H, m), 6.9–8.0 (50 H, py-3, py-4, py-5, Ph–Ph–, m), 8.3 (4 H, py-6, br d). IR (Nujol): 1720 ($C=O$, s), 839 (PF_6^-, s, br) cm^{-1}.

$[Cu_2(N5)(PPh_3)_2](PF_6)_2$ (5d$(PF_6)_2$). The synthesis and purification of this compound was performed in a manner analogous to that of $[Cu_2(N3)(PPh_3)_2](ClO_4)_2$ (**5a**$(ClO_4)_2$). The final yield was 60%. Anal. Calcd for $C_{69}H_{72}Cu_2F_{12}N_6P_4$: C, 56.59; H, 4.96; N, 5.74. Found: C, 55.10; H, 5.14; N, 5.52. ^1H NMR (CD_2Cl_2): δ 0.85–1.35 (6 H, br m), 2.30–3.10 (20 H, br m), 7.0–7.9 (42 H, py-3, py-5, PPh_3, br m), 8.10–8.40 (4 H, py-6, br d). IR (Nujol): 1605 ($C=C$, s), 1570 ($C=C$, s), 840 (PF_6^-, s, br) cm^{-1}.

Reactions of CO with $[Cu_2(N3)(O_2)](ClO_4)_2$ (2a$(ClO_4)_2$) and $[Cu_2(N3OR)(O_2)](PF_6)_2$ (2b$(PF_6)_2$) To Give $[Cu_2(N3)(CO)_2](ClO_4)_2$ (4a$(ClO_4)_2$) and $[Cu_2(N3OR)(CO)_2](PF_6)_2$ (4b$(PF_6)_2$). Crystalline samples of $[Cu_2(N3)(CH_3CN)_2](ClO_4)_2$ (**3a**$(ClO_4)_2$) (0.100 g, 0.111 mmol) and $[Cu_2(N3OR)](PF_6)_2\cdot CH_2Cl_2$ (**1b**$(PF_6)_2\cdot CH_2Cl_2$) (0.250 g, 0.209 mmol) were initially dissolved with stirring in 30 and 40 mL of Ar-saturated CH_2Cl_2, respectively. In each case, the yellow solution obtained was cooled to −85 ± 5 °C using an acetone/N_2 slush bath, and O_2 was bubbled through the solution for 7–10 min as the solution changed from a yellow to a deep purple/brown color. The reaction mixture was alternatively evacuated and purged with Ar for 5–6 cycles to remove the excess dioxygen. Carbon monoxide was directly bubbled through the solution while occasionally being allowed to warm by removing the reaction flask from the cold bath for 30-s intervals. Within 1 h the solution of **2a**$(ClO_4)_2$ had turned a clear yellow color while a little greenish tinge resulted in the case of **2b**$(PF_6)_2$. Precipitation with diethyl ether afforded 0.095 g (98%) of a pale yellow crystalline product, **4a**$(ClO_4)_2$. Anal. Calcd for $C_{31}H_{38}Cl_2Cu_2N_6O_{10}$: C, 45.21; H, 4.37; N, 9.59. Found: C, 45.27; H, 4.39; N, 9.93. In the latter case CO-saturated diethyl ether (about 25 mL) was added to the cloud point, and the solution was filtered under Ar through a medium-porosity frit, which resulted in a clear yellow solution and a very small amount of green precipitate. More diethyl ether (150 mL) saturated with CO was added to precipitate the product. The solution was then stirred producing an off-white fine powder, 0.20 g (78%, based on the production of a CH_2Cl_2 and Et_2O solvated complex[14b]). Upon recrystallization from $MeOH-Et_2O$ (1:5, v/v) under a CO atmosphere a microcrystalline material was obtained as a yellow-white solid, **4b**$(PF_6)_2$ (0.134 g, 55%). Anal. Calcd for $C_{46}H_{46}Cu_2F_{12}N_6O_4P_2$: C, 47.46; H, 3.95; N, 7.22. Found: C, 46.72; H, 4.08; N, 7.50. ^1H NMR (CD_3NO_2): δ 3.16 (20 H, br s), 6.8–7.95 (20 H, py-3, py-4, py-5, Ph–Ph–, m), 8.28 (4 H, py-6, br d). IR (Nujol): 2073 ($C=O$, s), 1718 (CO, s), 833 (PF_6^-, s, br) cm^{-1}.

Determination of O_2 Liberation from $[Cu_2(N\mathit{n})(O_2)]^{2+}$. Qualitative Methods. Application of a Vacuum or Reaction of CO with the Dioxygen Complexes. These experiments were performed in the same manner as described previously.[2a,11] A distinctive change in the color of the pyrogallol test solution from colorless to dark brown indicated the liberation of O_2 from the dioxygen complexes **2a** and **2b**. Careful control experiments showed no color change occurred unless the bound O_2 was removed by application of a vacuum or by displacement with CO.[14]

Quantitative Methods. The procedure utilizes a gravimetric method of O_2 determination which has been briefly outlined previously (footnote 50, ref 2a). Here, the O_2 given off upon application of vacuum and brief heating of a −80 °C CH_2Cl_2 solution of $[Cu_2(N4)(O_2)]^{2+}$ (**2c**) or $[Cu_2(N3OR)(O_2)]^{2+}$ (**2b**) (generated in situ from **1c**[2a] or **1b**) was trapped in a gas storage bulb at −196 °C. This bulb was then attached to another flask containing an excess of a CH_2Cl_2 solution of the dicopper(I) complex $[Cu_2(QPY2)(CH_3CN)_2](PF_6)_2$ (**6**), which is known to react in a reproducible manner with O_2 directly producing a precipitate with composition $\{Cu_2(QPY2-2H+O)Cl_2\}(PF_6)_2$ (**7**), $C_{36}H_{38}Cl_2Cu_2F_{12}N_6O_2P_2$ (4Cu:O_2, manometry).[15] Filtering under Ar and drying and weighing the amount of **7** produced then gives a measure of the amount of dioxygen trapped from the complexes $[Cu_2(N\mathit{n})(O_2)]^{2+}$. Using this method, 0.0540 g (0.0503 mmol) of **7** was obtained from 0.0361 g (0.0303 mmol) of **1b**$(PF_6)_2$, indicating that 83% of the O_2 expected from **2b**$(PF_6)_2$ was recovered by this procedure. Similarly, 82% was recovered in the case of $[Cu_2(N4)(O_2)]^{2+}$.[2a] The material balance in this procedure was

---

(14) (a) Haka, M. S. Ph.D. Thesis, State University of New York at Albany, 1987. (b) Farooq, A. Ph.D. Thesis, State University of New York at Albany, 1987.

(15) Karlin, K. D.; Cohen, B. I.; Farooq, A.; Liu, S.; Zubieta, J. *Inorg. Chim. Acta* **1988**, *153*, 9–11.

determined to be good, as indicated by weighing the compound **7** further produced by O_2 exposure of the excess amount of **6** in the filtrate. Further details can be found elsewhere.[14]

CO_2 Detection. The procedure followed is as previously described.[2a] No detectable precipitate formed in the test aqueous solution of $Ba(OH)_2$, upon passage of CO through the solutions of dioxygen complexes **2a** and **2b**.

Reactions of O_2 Complexes with Triphenylphosphine. Reactions of $[Cu_2(Nn)(O_2)]^{2+}$ with PPh_3 are very sluggish and require an excess of added phosphine to effect the conversion to both bis(triphenylphosphine) complexes **5** and triphenylphosphine oxide. For example, 0.194 g (0.163 mmol) of **1b**$(PF_6)_2$ was reacted with dioxygen at −80 °C in CH_2Cl_2 to produce $[Cu_2(N3OR)(O_2)]^{2+}$ (**2b**), excess O_2 was removed, and 0.0961 g (0.366 mmol) of PPh_3 was added. Stirring overnight and allowing the solution to warm to room temperature produced 0.07 g (26% yield) of $[Cu_2(N3OR)(PPh_3)_2](PF_6)_2$ (**5b**$(PF_6)_2$ (**5b**$(PF_6)_2$) upon precipitation with Et_2O. Gas chromatographic analysis of the ether washings showed that the product consisted of a 40:60 (wt %) mixture of PPh_3 and $O{=}PPh_3$ by weight, indicating that, of the 2.25 mol of PPh_3 that reacted/mol of $Cu_2{-}O_2$ complex, 1.31 mol was converted to $O{=}PPh_3$.[14b]

NMR Spectroscopy of O_2 Complexes. NMR spectra were taken in CD_3NO_2, CD_3COCD_3, $CDCl_3$, or CD_2Cl_2 on either a Varian EM360 (60 MHz) or a Varian XL-300 (300 MHz) NMR spectrometer. Chemical shifts are reported as δ values downfield from an internal standard of Me_4Si.

Typically, 50–100 mg of copper complexes was dissolved in 1 mL of CD_2Cl_2 in an Ar-filled glovebox. Complexes **4a**$(PF_6)_2$ and **4d**$(PF_6)_2$ are not highly soluble in CD_2Cl_2, so only complexes **1b**$(PF_6)_2{\cdot}CH_2Cl_2$ and **3a**$(ClO_4)_2$ could be studied. Wilmad NMR tubes (Model 528-JY, 5-mm o.d. with special rotary valve) were used in these experiments. Spectra of complexes **1b**$(PF_6)_2{\cdot}CH_2Cl_2$ and **3a**$(ClO_4)_2$ were taken at room temperature initially to confirm that the starting complex was pure. The instrument probe temperature was lowered to −85 °C and the spectrum recorded. The sample tube was then placed into a cold bath (acetone/N_2 at −90 °C) and attached to the vacuum line. The copper(I) solution was evacuated, and O_2 was admitted to this solution at −90 °C. The valve was closed, the tube was inverted and shaken, and the vacuum/O_2 cycles were repeated three times over 15 min resulting in the development of a color change to an intense brown color (**1b**$(PF_6)_2{\cdot}CH_2Cl_2$) or purple (**3a**$(ClO_4)_2$). The excess O_2 was then removed with several vacuum/Ar-purge cycles, the rotary valve was closed, and the sample tube was replaced into the cold NMR instrument probe.

Gas (O_2 and CO) Uptake Measurements. For complexes **1a**$(ClO_4)_2$, **3a**$(ClO_4)_2$, and **1b**$(PF_6)_2$, measurements of the uptake of dioxygen or carbon monoxide at temperatures varying from room temperature to −80 °C were carried out using a gas buret system as described in ref 2a. This method applies for samples in which the solids are unreactive toward O_2 but which react readily with O_2 in solution. The gas uptake measurements for decarbonylated solutions of $[Cu_2(N3)(CO)_2](PF_6)_2$ (**4a**$(PF_6)_2$) and $[Cu_2(N5)(CO)_2](PF_6)_2$ (**4d**$(PF_6)_2$) were carried out by methods described previously.[2a,11]

The stoichiometry of the uptake of dioxygen using ca. 0.5 mmol of the dicopper(I) complexes **1a**, **3a**, **4a**, **1b**, and **4d** at −80 °C was as follows: $[Cu_2(N3)](ClO_4)_2$ (**1a**$(ClO_4)_2$), 2:0.96 Cu:O_2 (1 trial); $[Cu_2(N3OR)](PF_6)_2$ (**1b**$(PF_6)_2$), 2:0.93 (±0.01) Cu:O_2 (2 trials); $[Cu_2(N3)(CH_3CN)_2](ClO_4)_2$ (**3a**$(ClO_4)_2$), 2:0.98 (±0.02) Cu:O_2 (3 trials); $[Cu_2(N3)(CO)_2](ClO_4)_2$ (**4a**$(ClO_4)_2$), 2:0.87 (±0.03) Cu:O_2 after decarbonylation (3 trials); $[Cu_2(N5)(CO)_2](PF_6)_2$ (**4d**$(PF_6)_2$), 2:0.89 Cu:O_2 after decarbonylation (1 trial). The uptake of CO at room temperature by 0.5082 g (0.4263 mmol) of $[Cu_2(N3OR)](PF_6)_2$ (**1b**$(PF_6)_2$) was found to be 0.8021 mmol for the formation of compound $[Cu_2(N3OR)(CO)_2](PF_6)_2$ (**4b**$(PF_6)_2$) (i.e. Cu:CO = 2:2). The observed Cu:CO stoichiometry of the reaction in CH_2Cl_2 at 0 °C for complex $[Cu_2(N3)(CH_3CN)_2](ClO_4)_2$ (**3a**$(ClO_4)_2$) was found to be 2:1.60 Cu:CO.

Electrochemistry. The electrochemical cell consisted of a modification of a standard three-chambered design equipped for handling air-sensitive solutions by utilizing high vacuum valve (Viton O-ring) seals. Either a platinum disk (BAS MF 2013) or glassy-carbon electrode (GCE, BAS MF 2012) was used as the working electrode. Electrode preparation and cleaning consisted of sequential washing with 6 M HNO_3, water, and acetone for the Pt electrode and polishing the GCE with a gem polish slurry on a felt cloth, followed by washing with acetone. The reference electrode used was a Ag/AgCl Metrohm Model 6.0724.140, stored in 0.1 M tetrabutylammonium hexafluorophosphate (TBAHP) and saturated $LiCl{-}CH_2Cl_2$ solution. It was placed in the compartment solution separated from the working solution by means of a fine glass frit. The auxiliary electrode consisted of a coiled platinum wire. At the bottom of the chamber and directly underneath the working electrode was a cube-shaped platinum net with connection sealed to the soft glass on the side. This cell design allowed for cyclic voltammetry (CV) and bulk electrolysis (coulometry) to be carried out on the same sample. The working and reference electrode fritted tips were placed as close as possible to each other to minimize solution *IR* drop. The TBAHP supporting electrolyte concentration was 200 times (~0.2 M) that of the solute (~10^{-3} M) being studied.

Table I. Crystallographic Data for Bis(carbonyl) Complex **4a**$(ClO_4)_2$

formula	$C_{33}H_{38}Cl_2Cu_2N_6O_{10}$
temp, K	294
MW	876.69
cryst system	monoclinic
space group	$P2_1/n$
a, Å	10.255 (2)
b, Å	25.943 (3)
c, Å	14.767 (3)
α, deg	90.00
β, deg	94.94 (1)
γ, deg	90.00
V, Å^3	3914.2 (10)
$F(000)$	1800
Z	4
D_{calcd}, g/cm^3	1.49
abs coeff, cm^{-1}	12.87
no. of reflcns collcd	5723
no. of indpt reflcns	2659 ($\geq 6\sigma|F_o|$)
no. of refined params (N_v)	275
largest peak/hole, e Å^{-3}	0.79/−0.51
R^a	0.0781
$R_w{}^b$	0.0836

$^a R = \sum[|F_o| - |F_c|/\sum|F_o|]$. $^b R_w = [\sum w(|F_o| - |F_c|)^2/\sum w|F_o|^2]^{1/2}$; $w = 1/\sigma^2(F_o) + g(F_o)^2$; $g = 0.001$.

CV and coulometric experiments were carried out using a BAS CV 27 instrument and Houston Instruments Model 100 X-Y recorder. Scan rates of 50–500 mV/s were generally employed, and the ferrocene/ferrocenium (Fc/Fc$^+$) couple ($E_{1/2}$ = 0.55 V vs NHE) was used as calibrant: Measured values were ΔE_p = 60 mV, $E_{1/2}$ = 0.55 V (DMF), and $E_{1/2}$ = 0.67 V (CH_2Cl_2) vs the Ag/AgCl reference electrode used. For low-temperature measurements, the cell was immersed in a dry ice (and/or N_2)/acetone slush bath and the temperature was monitored using an OMEGA, Inc., Model 670 resistance thermometer. Some precipitation of TBAHP was observed at −80 to −90 °C, but this did not affect the nature of the CV as judged using the Fc/Fc$^+$ reference.

X-ray Crystallography. Crystallization, Collection, and Reduction of X-ray Diffraction Data. A dichloromethane–diethyl ether solution of compound $[Cu_2(N3)(CO)_2](ClO_4)_2$ (**4a**$(ClO_4)_2$) under Ar at room temperature yielded clear yellow crystals of that were suitable for X-ray crystallographic analysis. An epoxy-covered crystal was mounted on a Nicolet R3m four-circle automated diffractometer with a Mo X-ray source equipped with a highly ordered graphite monochromator (λ(Mo Kα) = 0.710 73 Å). Automatic centering and least-squares routines were carried out on 25 reflections to obtain the cell dimensions that are given in Table I. A coupled θ(crystal) to 2θ(counter) scan mode was employed. The scan length was $(2\theta(K\alpha_1 - 1.0)$ to $2\theta(K\alpha_2 - 1.0))°$. Three check reflections were measured every 197 reflections; these exhibited no significant decay during data collection. The program XTAPE of the SHELXTL package[16] was used to process the data. A summary of cell parameters, data collection parameters, and refinement results for complex **4a**$(ClO_4)_2$ is found in Table I.

Structure Solution and Refinement. The positional parameters of the copper atoms were determined by the Patterson method. The remaining non-hydrogen atoms were located by subsequent difference Fourier maps and least-square refinements. Atomic scattering factors for neutral atoms were used throughout the analysis. Complex **4a**$(ClO_4)_2$ crystallizes in the monoclinic space group $P2_1/n$ with Z = 4. Each asymmetric unit is found to contain one complete molecule. Anisotropic refinement was carried out on the copper atoms, the carbonyl ligands, the nitrogen atoms, and all atoms in the anions. The pyridine rings were refined as rigid groups, and all remaining atoms were refined isotropically. The hydrogen atoms were included at calculated positions in the final stages of refinement with their thermal parameters constrained to be 1.2 times those of the carbons to which they were bonded and not refined. The large thermal motions of atoms in the perchlorate anions, especially the anion

---

(16) All calculations were performed on a Data General Nova 3 computer with 32 K of 16-bit words using local versions of the Nicolet SHELXTL interactive crystallographic software package, as described in: Sheldrick, G. M., *Nicolet SHELXTL Operations Manual*; Nicolet XRD Corp: Cupertino, CA, 1979.

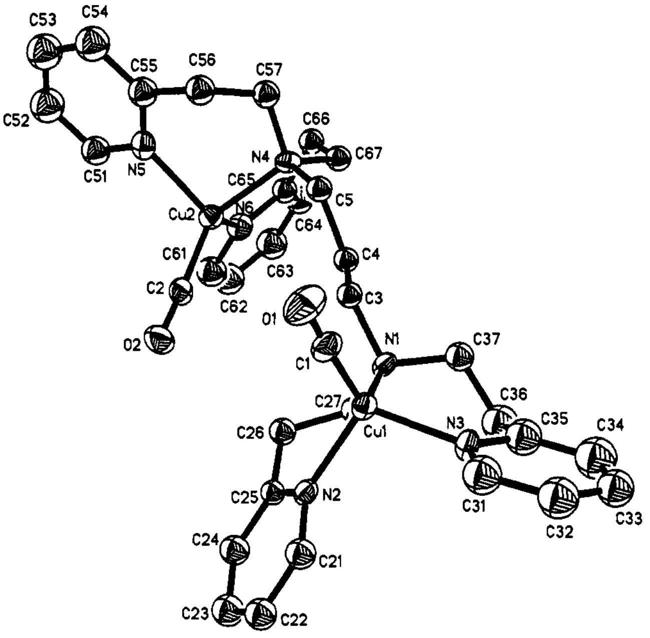

Figure 2. ORTEP diagram of the cationic portion of the bis(carbonyl) adduct $[Cu_2(N3)(CO)_2](ClO_4)_2$ ($4a(ClO_4)_2$), showing the atom-labeling scheme.

consisting of Cl2, O7, O8, O9, and O10, are likely indicative of disorder involving these atoms; no attempt was made to model or resolve this disorder.

The final *R* factor, crystal data, and details of the data collection and refinement procedures are given in Tables I (short version) and VI (supplementary material). Structure factors, bond lengths, bond angles, anisotropic temperature factors, and hydrogen coordinates and temperature factors are available in the supplementary material (Tables VII–XI).

Results and Discussion

Synthesis of Dicopper Complexes. As previously discussed,[1,2a] the use of the hydrocarbon-linked dinucleating ligands L evolved out of the chemistry developed with the ligand XYL-H, in which a *m*-xylyl group connects two PY2 tridentates (Figure 1). Copper(I) readily forms tricoordinate complexes with PY2, and tetracoordinate adducts with additional ligands such as RCN, CO, and PPh_3 are also readily prepared. One of our first accomplishments in this area involved the characterization of $[Cu_2(XYL)]^{2+}$, with two such moieties in a dinuclear unit.[4] This complex provides a wealth of interesting bioinorganic model chemistry for (a) it can serve as a crude model for deoxy-Hc or -Tyr, (b) the reaction of $[Cu_2(XYL\text{-}H)]^{2+}$ (**1e**) with O_2 provides a tyrosinase model system (vide supra),[4] and (c) $[Cu_2(XYL\text{-}O\text{-})]^+$ reacts reversibly with O_2 in dichloromethane at low temperature to give a peroxodicopper(II) complex $[Cu_2(XYL\text{-}O\text{-})(O_2)]^+$ (discussed further below).[11b]

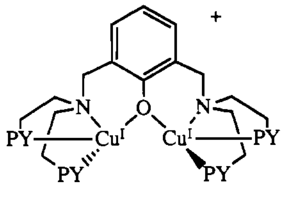

$[Cu_2{}^I(XYL\text{-}O\text{-})]^+$

Closely related to the reactions of $[Cu(XYL\text{-}H)]^{2+}$ (**1e**) are the N*n* systems with PY2 ligands which are hydrocarbon $-(CH_2)_n-$ linked. These form another class of dicopper(I) complexes $[Cu^I_2(Nn)]^{2+}$ (**1**) or $[Cu^I_2(Nn)(CH_3CN)_2]^{2+}$ (**3**), which also react reversibly with CO and O_2 (Figure 1). In addition to the ligand N4 ($n = 4$),[2a] those with L = N3, N3OR, and N5 were chosen in order to provide a series of dinuclear complexes for which we could examine the possible consequences caused by variations in local microenvironment and Cu$\cdots$Cu distance (or interactions) upon reaction chemistry. Differences in the chemistry as a function of L are in fact apparent (vide infra). Tricoordinate complexes, $[Cu^I_2(Nn)]^{2+}$ (**1**), can be isolated as pure solids from the reaction of 2 equiv of $[Cu(CH_3CN)_4]Y$ ($Y = PF_6^-, ClO_4^-$) with N3, N3OR, or N4 in CH_2Cl_2. The initial products for L = N3 and N4 are the bis(acetonitrile) adducts $[Cu^I_2(Nn)(CH_3CN)_2]^{2+}$ (**3**), in which CH_3CN is strongly bound (see Experimental Section). The N3OR ligand was designed to be a close analogue of N3 but with a large biphenylcarbonyl organic group present to potentially improve the solubility and/or crystallinity of derived complexes. In fact, these expectations were realized; the structure of $[Cu^I_2(N3OR)]^{2+}$ (**1b**) shows separated tricoordinate Cu(I) moieties with Cu$\cdots$Cu = 6.262 Å.[2d]

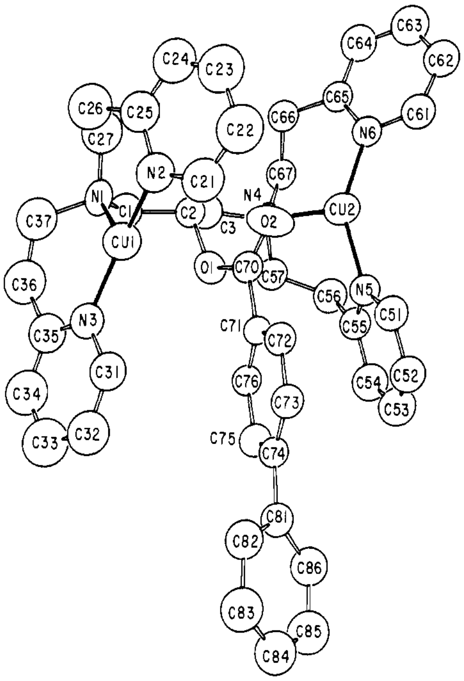

In contrast to what is observed for L = N3 and N4, a bis(acetonitrile) adduct of **1b** does not form under similar synthetic conditions. The CO and PPh_3 adducts $[Cu^I_2(L)(L')_2]^{2+}$ (L′ = CO (**4**), ν_{CO} (Nujol) = 2073–2095 cm^{-1}; L′ = PPh_3 (**5**)) readily form for all three ligands (Figure 1). Manometric CO uptake measurements performed on **1b** (Experimental Section) are consistent with the bisadduct formation. Carbon monoxide can displace coordinated acetonitrile as indicated by a manometric CO uptake experiment carried out on $[Cu^I_2(N3)(CH_3CN)_2]^{2+}$ (**3a**) in CH_2Cl_2. These observations suggest that the qualitative order of binding strength is $CH_3CN < CO < PPh_3$, in accord with that found for the N4 ligand.[2a] With the N5 ligand, only $[Cu^I_2(L)(CO)_2]^{2+}$ (**4d**) and $[Cu^I_2(L)(PPh_3)_2]^{2+}$ (**5d**) were stable as solids and neither a tricoordinate dicopper(I) complex nor a bis(acetonitrile) adduct could be isolated. These may be generated in situ, however; i.e., $[Cu^I_2(N5)]^{2+}$ (**1d**) was obtained by decarbonylation (in vacuo) of solutions of **4d**.

$$\underset{\mathbf{1}}{[Cu^I_2(L)]^{2+}} + 2L' \rightarrow \begin{array}{c}[Cu^I_2(L)(L')_2]^{2+}\\ L' = CH_3CN\ (\mathbf{3})\\ L' = CO\ (\mathbf{4})\\ L' = PPh_3\ (\mathbf{5})\end{array}$$

The IR absorption frequencies of the coordinated CO molecules in **4a–c** (ν_{CO} = 2073–2095 cm^{-1}; see Experimental Section) are typical[17-25] of terminally coordinated CO in copper(I) carbonyl

---

(17) Pettingill, T. M.; Strange, R. W.; Blackburn, N. J. *J. Biol. Chem.* **1991**, *266*, 16996–17003.

(18) Patch, M. G.; Choi, H.; Chapman, D. R.; Bau, R.; McKee, V.; Reed, C. A. *Inorg. Chem.* **1990**, *29*, 110–119.

(19) Villacorta, G. M.; Lippard, S. J. *Inorg. Chem.* **1987**, *26*, 3672–3676. A compilation of structural parameters for Cu(I)–CO complexes is provided in this reference.

Table II. Atom Coordinates (×10^4) and Temperature Factors (Å^2 × 10^3) for Compound $[\mathrm{Cu^I_2(N3)(CO)_2}](\mathrm{ClO_4})_2$ (**4a**$(\mathrm{ClO_4})_2$)[a]

atom	*x*	*y*	*z*	$U_{\mathrm{equiv/iso}}$
Cu1	−2309 (1)	3298 (1)	7248 (1)	55 (1)
Cu2	1535 (2)	1072 (1)	7495 (1)	61 (1)*
C1	−2750 (14)	3186 (5)	6050 (9)	77 (6)*
O1	−2970 (12)	3123 (4)	5299 (7)	119 (5)*
C2	−71 (12)	1131 (4)	7873 (10)	72 (6)*
O2	−1070 (10)	1144 (4)	8127 (8)	110 (5)*
N1	−499 (8)	3046 (4)	7848 (6)	55 (4)*
N4	2507 (9)	1635 (4)	6810 (6)	54 (4)*
C3	16 (11)	2691 (4)	7161 (7)	58 (3)
C4	1261 (11)	2374 (5)	7458 (8)	58 (3)
C5	1727 (11)	2104 (5)	6636 (8)	61 (4)
C21	−4694 (7)	3218 (3)	8206 (5)	75 (4)
C22	−5541 (7)	3022 (3)	8812 (5)	81 (4)
C23	−5160 (7)	2604 (3)	9366 (5)	87 (5)
C24	−3931 (7)	2381 (3)	9315 (5)	77 (4)
C25	−3083 (7)	2576 (3)	8709 (5)	52 (3)
N2	−3465 (7)	2994 (3)	8155 (5)	59 (4)*
C26	−1772 (11)	2377 (5)	8620 (9)	66 (4)
C27	−693 (11)	2761 (5)	8707 (8)	63 (4)
C31	−3099 (7)	4385 (4)	7178 (6)	113 (6)
C32	−2979 (7)	4918 (4)	7273 (6)	122 (6)
C33	−1872 (7)	5129 (4)	7750 (6)	102 (5)
C34	−884 (7)	4806 (4)	8131 (6)	139 (7)
C35	−1004 (7)	4273 (4)	8036 (6)	107 (5)
N3	−2111 (7)	4062 (4)	7560 (6)	62 (4)*
C36	−157 (17)	3906 (6)	8591 (12)	119 (6)
C37	389 (12)	3492 (5)	8012 (9)	72 (4)
C51	1713 (8)	−18 (4)	6899 (5)	91 (5)
C52	1733 (8)	−424 (4)	6281 (5)	123 (6)
C53	1759 (8)	−322 (4)	5355 (5)	129 (7)
C54	1765 (8)	187 (4)	5047 (5)	116 (6)
C55	1745 (8)	593 (4)	5665 (5)	84 (5)
N5	1719 (8)	490 (4)	6591 (5)	73 (5)*
C56	1773 (14)	1141 (5)	5432 (9)	81 (4)
C57	2809 (13)	1448 (5)	5909 (9)	71 (4)
C61	2495 (7)	654 (4)	9270 (7)	102 (5)
C62	3393 (7)	538 (4)	10006 (7)	117 (6)
C63	4699 (7)	685 (4)	9992 (7)	117 (6)
C64	5108 (7)	948 (4)	9243 (7)	89 (5)
C65	4210 (7)	1064 (4)	8507 (7)	70 (4)
N6	2904 (7)	917 (4)	8521 (7)	76 (5)*
C66	4607 (12)	1315 (5)	7708 (8)	69 (4)
C67	3766 (12)	1778 (5)	7360 (8)	66 (4)
Cl1	7168 (4)	1606 (2)	5868 (3)	68 (1)*
Cl2	8352 (5)	1156 (3)	968 (4)	138 (3)*
O3	6375 (13)	1191 (5)	5871 (10)	149 (7)*
O4	6923 (12)	1927 (5)	6549 (9)	150 (7)*
O5	6991 (14)	1835 (7)	5056 (10)	192 (9)*
O6	8464 (12)	1468 (6)	5927 (10)	163 (8)*
O7	9494 (21)	1340 (14)	1013 (19)	422 (22)*
O8	7509 (25)	1477 (9)	700 (23)	384 (21)*
O9	8346 (31)	987 (11)	1700 (16)	367 (20)*
O10	8114 (28)	819 (12)	339 (19)	411 (22)*

[a] Asterisks indicate values of equivalent isotropic *U* defined as one-third of the trace of the orthogonalized $\mathbf{U}_{ij}$ tensor.

Table III. Selected Bond Distances and Angles for Compound **4a**$(\mathrm{ClO_4})_2$

Bond Distances (Å)			
Cu1–N1	2.092 (9)	Cu2–N5	2.033 (9)
Cu1–N2	2.023 (8)	Cu2–N6	2.015 (8)
Cu1–N3	2.040 (10)	Cu2–C2	1.792 (13)
Cu1–C1	1.811 (14)	C1–O1	1.124 (17)
Cu2–N4	2.080 (9)	C2–O2	1.120 (17)
Bond Angles (Deg)			
N1–Cu1–N2	98.4 (3)	N1–Cu1–C1	120.1 (5)
N1–Cu1–N3	98.1 (3)	N2–Cu1–C1	118.2 (5)
N2–Cu1–N3	106.4 (3)	N3–Cu1–C1	112.9 (5)
N4–Cu2–N5	97.3 (3)	N4–Cu2–C2	125.7 (5)
N4–Cu2–N6	100.0 (4)	N5–Cu2–C2	114.1 (5)
N5–Cu2–N6	104.4 (4)	N6–Cu2–C2	112.5 (5)

compounds. As was the case for $[\mathrm{Cu^I_2(N4)(CH_3CN)_2}]^{2+}$,[2a] no ν_{CN} is observed for the coordinated acetonitrile molecule in $[\mathrm{Cu^I_2(N3)(CH_3CN)_2}]^{2+}$ (**3a**); we have observed this vibration at 2240 cm^{-1} for another PY2-containing dicopper(I) complex,[26] and ν_{CN} is found in the range 2280–2310 cm^{-1} for a dinuclear tetracoordinate compound containing the $\mathrm{LCu^I{-}CH_3CN}$ moiety (L = an amine–bis(thioether) tridentate ligand).[27]

Dicopper(I) Bis(carbonyl) Adducts and the Structure of $[\mathrm{Cu^I_2(N3)(CO)_2}](\mathrm{ClO_4})_2$ (4a$(\mathrm{ClO_4})_2$). There has been increased interest in carbonyl complexes of Cu(I) in the last few years,[17-25] with potential use in gas separation processes, possible organometallic activation of CO, and bioinorganic modeling. Carbon monoxide as a ligand has the ability to stabilize copper ion in the +1 oxidation state, and CO is of interest as a probe of Cu(I) sites in proteins.[2d,17,18,24] Also, a curious behavior of deoxyhemocyanin is that it binds only 1 mol of CO/dinuclear Cu(I) complex.[28] We generate CO-stabilized Cu(I) complexes as precursors for dioxygen–Cu(I) reactivity studies. The coordination of CO to the tricoordinate Cu(I) dinuclear compounds $[\mathrm{Cu^I_2(N}n)]^{2+}$ (**1**) is reversible, and CO can displace bound dioxygen from $[\mathrm{Cu_2(N}n)(\mathrm{O_2})]^{2+}$ (**2**) (vide infra).

A summary of crystal and refinement data for **4a**$(\mathrm{ClO_4})_2$ is given in Table I, with final positional parameters provided in Table II; selected bond distances and angles are found in Table III. Its structure consists of the $[\mathrm{Cu^I_2(N3)(CO)_2}]^{2+}$ dication and well-separated perchlorate anions. Figure 2 shows the structure of the dication, where the copper coordination units are separated from each other with Cu···Cu = 6.986 (2) Å. The Cu(I) ions are found in a very similar pseudotetrahedral geometries coordinated to two pyridyl and one amino nitrogen atoms from the PY2 tridentate group, along with the CO ligand. The dihedral angles are near the expected value of 90° and vary from 84.2 to 94.6° (e.g. N1–Cu1–N2/N3–Cu1–C1 = 94.0°; N2–Cu1–N3/N1–Cu1–C1 = 89.1°; N2–Cu1–C1/N1–Cu1–N3 = 84.9°). Both Cu1 and Cu2 atoms sit 0.93–0.94 Å out of the plane of the three nitrogen donors. This pseudotetrahedral description is similar to that found for the closely related $[\mathrm{Cu^I_2(N4)(CH_3CN)_2}]^{2+}$ complex[2a] and conforms with other tetracoordinate Cu(I) structures containing tetradentate ligand donors which include the PY2 unit. These latter structures are better described as trigonal pyramidal, where the amine N is in the apical position and the Cu ion sits within ~0.3 Å of the plane including the pyridyl N atoms and another nitrogen or oxygen donor ligand.[11b,29] Here, the pseudotetrahedral moieties are elongated in the direction of the Cu–CO axes, as indicated by the difference between the chelating N–Cu–N angles

---

(20) Thompson, J. S.; Whitney, J. F. *Inorg. Chem.* **1984**, *23*, 2813.

(21) Gagné, R. R.; Kreh, R. P.; Dodge, J. A.; Marsh, R. E.; McCool, M. *Inorg. Chem.* **1982**, *21*, 254–261.

(22) Kläui, W.; Lenders, B.; Hessner, B.; Evertz, K. *Organometallics* **1988**, *7*, 1357–1363.

(23) (a) Pasquali, M.; Floriani, C.; Gaetani-Manfredotti, A.; Guastini, C. *J. Am. Chem. Soc.* **1981**, *103*, 185. (b) Pasquali, M.; Floriani, C.; Venturi, G.; Gaetani-Manfredotti, A.; Chiesi-Villa, A. *J. Am. Chem. Soc.* **1982**, *104*, 4092. (c) Doyle, G.; Eriksen, K. A.; Modrick, M.; Ansell, G. *Organometallics* **1982**, *1*, 1613–1618. (d) Pasquali, M.; Floriani, C.; Geatani-Manfredotti, A. *J. Chem. Soc., Chem. Commun.* **1978**, 921.

(24) (a) Sorrell, T. N.; Jameson, D. L. *J. Am. Chem. Soc.* **1982**, *104*, 2053. (b) Sorrell, T. N.; Borovik, A. S. *Inorg. Chem.* **1987**, *26*, 1957–1964. (c) Sorrell, T. N.; Borovik, A. S. *J. Am. Chem. Soc.* **1987**, *109*, 4255–4260.

(25) (a) Kimura, E.; Koike, T.; Kodama, M.; Meyerstein, D. *Inorg. Chem.* **1989**, *28*, 2998–3001. (b) Casella, L.; Gullotti, M.; Pallanza, G.; Rigoni, L. *J. Am. Chem. Soc.* **1988**, *110*, 4221–4227. (c) Balkus, K. J., Jr.; Kortz, A.; Drago, R. S. *Inorg. Chem.* **1988**, *27*, 2955–2958. (d) Kitagawa, S.; Munakata, M. *Inorg. Chem.* **1981**, *20*, 2261.

(26) Karlin, K. D.; Ghosh, P.; Cruse, R. W.; Farooq, A.; Gultneh, Y.; Jacobson, R. R.; Blackburn, N. J.; Strange, R. W.; Zubieta, J. *J. Am. Chem. Soc.* **1988**, *110*, 6769–6780.

(27) Karlin, K. D.; Hayes, J. C.; Hutchinson, J. P.; Zubieta, J. *Inorg. Chim. Acta* **1983**, *78*, L45–L46.

(28) (a) Alben, J. O.; Yen, L.; Farrier, N. J. *J. Am. Chem. Soc.* **1970**, *92*, 4475–4476. (b) Yen-Fager, L.; Alben, J. O. *Biochemistry* **1972**, *11*, 4786–4792.

(29) Karlin, K. D.; Hayes, J. C.; Hutchinson, J. P.; Hyde, J. R.; Zubieta, J. *Inorg. Chim. Acta* **1982**, *64*, L219–L220.

(N_{amine}–Cu–N_{py} = 98.5° (average) and N_{py}–Cu–N_{py} = 105.4° (average)) and the larger N–Cu–C(O) angles (112.5–120.1°) (Table III).

The Cu–N bond lengths in **4a**(ClO_4)$_2$ are normal and similar to Cu–N_{amine} and Cu–N_{py} distances observed in other tetracoordinater Cu(I) complexes such as $[Cu^I_2(N4)(CH_3CN)_2]^{2+}$[2a] and $[Cu(tepa)]^+$ (tepa = tris(2-(2-pyridyl)ethyl)amine).[29] Interestingly, the Cu–N_{amine} bond lengths (2.08, 2.09 Å) are shorter than those observed for three-coordinate Cu(I) complexes with the PY2 tridentate (2.16–2.22 Å),[2d,4,30a] while the Cu–N_{py} distances (2.01–2.04 Å) are more than 0.1 Å longer than corresponding bond lengths in these three-coordinate complexes (1.87–1.94 Å). As previously discussed,[4] Cu(I)–N_{arom} (N_{arom} = pyridine, imidazole, pyrazole) bond lengths fall into distinct groups for complexes having two-, three-, or four-coordinate Cu(I) complexes. The copper carbonyl bonding parameters (e.g. Cu–CO, C–O, and ∠Cu–C–O) are typical for the other Cu(I)–CO complexes which have been structurally characterized.[18-23]

A close analogue of **4a**, $[Cu_2(TPEN)(CO)_2]^{2+}$ (TPEN = *N,N,N′,N′*-tetrakis(2-pyridylmethyl)ethylenediamine), has been described by Gagné and co-workers;[21] this also contains a N_3-Cu^I–CO cationic core, and the binding of CO to the dicopper(I) precursor is also reversible. The chelate ring sizes are smaller in $[Cu_2(TPEN)(CO)_2]^{2+}$, but the overall pseudotetrahedral geometry is rather similar. The larger bite angle possible in **4a** results in naturally larger angles about the amine nitrogen atoms, where for $[Cu_2(TPEN)(CO)_2]^{2+}$ the N_{amine}–Cu–N_{py} and N_{py}–Cu–N_{py} values average only 81.5 and 109.5°, respectively. The TPEN complexes also has ~0.1 Å longer Cu–N_{amine} bond lengths compared to **4a**, while the Cu–N_{py} bond distances are quite alike (2.03 Å (average)). Reed and co-workers[17] have more recently described a very comparable bis(carbonyl) structure also containing the N_3Cu^I–CO moiety but where the aromatic nitrogen donors are substituted benzimidazoles rather than pyridine. The coordinate geometry there is described as distorted trigonal pyramidal with an apical tertiary amine ligand. Compared to compound **4a** and $[Cu_2(TPEN)(CO)_2]^{2+}$, Reed's compound possesses very long Cu–N_{amine} bond distances, and most of the other bond angles around the copper ions vary considerably as well. The authors suggest that the distortions may arise from the presence of the sterically demanding bulky benzimidazole donors.

Overall, the structure observed here is fairly typical those seen for other copper(I) carbonyl complexes.[18-23] Both mono- and dinuclear Cu(I) complexes with CO ligands have been described, and the majority of structurally characterized Cu(I)–CO complexes contain linear terminally bound CO ligands with ν_{CO} in the range 2055–2117 cm^{-1} (here ν_{CO} (Nujol) = 2080 (**4a**), 2073 (**4b**), 2095 (**4d**) cm^{-1}). There are also a number of cases known where a CO ligand can bridge two Cu^+ ions (ν_{CO} = 1908–1926 cm^{-1}).[23a-c] The majority of the Cu(I)–CO complexes described possess overall tetracoordination having amine-type donors, although several of these cases include situations where one of the donors is a weakly coordinated anion such as ClO_4^- or BPh_4^-.[20,23d] Two-coordinate Cu(I) complexes have a very low affinity for CO,[24] but three-coordinate Cu(I) solution adducts having two N-donors plus a CO ligand have been proposed,[25b] and there is one structurally characterized example with trigonal coordination using an anionic tropocoronand ligand TC-5,5 in the dinuclear complex $[Cu_2(CO)_2(TC\text{-}5,5)]$.[19]

Low-Temperature Reactions of O_2 with Dicopper(I) Complexes. Genesis of $\{Cu_2–O_2\}$ Adducts $[Cu_2(Nn)(O_2)]^{2+}$ (2). The bis(carbonyl) adducts $[Cu_2(L)(CO)_2]^{2+}$ (**4**) serve as very useful and stable starting materials for reactivity studies. Their solutions can be readily decarbonylated at room temperature by the application of a vacuum, affording three-coordinate complexes $[Cu_2(L)]^{2+}$ (**1**). Pure samples of **1** can be prepared for L = N3, N3OR,[2d] and N4,[2a] and these along with bis(acetonitrile) adducts $[Cu_2(L)(CH_3CN)_2]^{2+}$ (L = N3 (**3a**); L = N4((**3c**)[2a]) serve as convenient precursors for dioxygen–copper adducts.

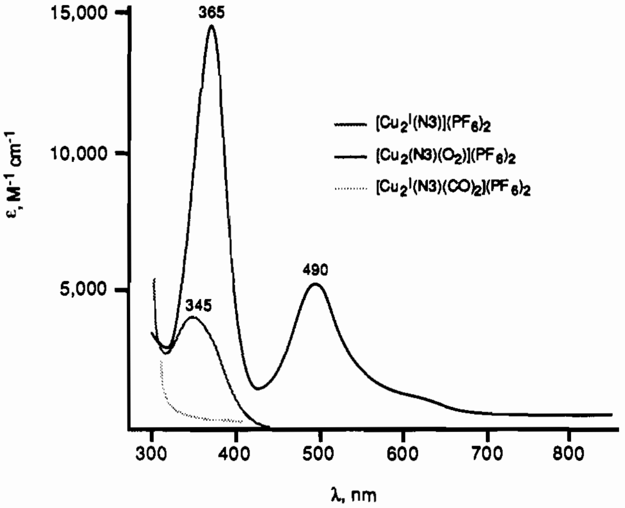

Figure 3. UV–vis spectra of the tricoordinate dicopper(I) complex $[Cu_2(N3)]^{2+}$ (**1a**), the bis(carbonyl) adduct $[Cu_2(N3)(CO)_2]^{2+}$ (**4a**), and the dioxygen adduct $[Cu_2(N3)(O_2)]^{2+}$ (**2a**).

As described previously,[2a] solutions of $[Cu_2(N4)]^{2+}$ (**1c**) or $[Cu_2(N4)(CH_3CN)_2]^{2+}$ (**3c**) react with dioxygen even at −80 °C in dichloromethane to give the dioxygen adducts $[Cu_2(N4)(O_2)]^{2+}$ (**2c**). The reactions with O_2 are extremely rapid even at this temperature, and the binding of O_2 appears to be immediate. The $\{Cu_2–O_2\}^{2+}$ species are highly colored and are characterized by multiple and strong absorptions in the UV–vis region; these adducts are stable only at these low temperature, and the absorptions disappear upon warming. The stoichiometry of O_2 binding for all of the complexes $[Cu_2(Nn)]^{2+}$ (**1**) is Cu:O_2 = 2:1 (manometry, −80 °C, see Experimental Section), i.e. one dioxygen per dicopper(I) complex. This stoichiometry is observed either when the three-coordinate species **1** or the bis(acetonitrile) adducts **3** are utilized. When the bis(carbonyl) adducts $[Cu_2(Nn)(CO)_2]^{2+}$ (**4**) are used as O_2-adduct precursors, somewhat less dioxygen is absorbed by the chilled and decarbonylated complex solutions of **4** (Experimental Section). This is attributed to the incomplete removal of CO from solutions of **4**, normally carried out by application of room-temperature vacuum/Ar-purge cycles.

UV-Vis Spectra. The most prominent UV–vis feature of these dioxygen complexes $[Cu_2(L)(O_2)]^{2+}$ (**2**) is the very strong absorption found in the 350–365-nm region, with observed molar extinction coefficients in the 15 000–21 500 M^{-1} cm^{-1} range depending on the particular dinucleating ligand L used. A summary and comparison of spectral and other data for $\{Cu_2–O_2\}^{n+}$ species is given in Table IV, and the spectra are shown for the N3 ligand complexes in Figure 3. Limitations imposed by the spectrometer and apparatus used for acquiring low-temperature UV–vis data precluded measurements below 315 nm; all complexes studied possess strong and increasing absorptions at the higher energies. The colorless bis(carbonyl) adduct $[Cu_2(N3)(CO)_2]^{2+}$ (**4**) gives a featureless spectrum, but upon decarbonylation or direct dissolution of $[Cu_2(N3)]^{2+}$ (**1a**), a spectrum with λ_{max} at 345 nm (Figure 3) is observed. Oxygenation of **1a** provides an intensely purple solution characterized by a strong 365-nm absorption (ϵ = 15 000 M^{-1} cm^{-1}) and a band at 490 nm (ϵ = 5250 M^{-1} cm^{-1}). In addition, there is a shoulder at ~600 (ϵ = 1200 M^{-1} cm^{-1}) and a much weaker absorption (ϵ ~ 100) is observed near 850 nm (not shown). The dioxygen adducts $[Cu_2(L)(O_2)]^{2+}$ (**2**) for L = N3OR, N4, and N5 are intensely brown in appearance, and while all the spectra possess strong band near 360 nm, the positions and intensities of the other absorption bands vary as a function of L (see further discussed below). UV–vis spectra for complexes containing the N3OR and N5 ligands appear below or in sup-

---

(30) (a) Blackburn, N. J.; Karlin, K. D.; Concannon, M.; Hayes, J. C.; Gultneh, Y.; Zubieta, J. *J. Chem. Soc., Chem. Commun.* **1984**, 939–940. (b) Karlin, K. D.; Gultneh, Y.; Hayes, J. C.; Zubieta, J. *Inorg. Chem.* **1984**, *23*, 519–521.

(31) Karlin, K. D.; Shi, J.; Hayes, J. C.; McKown, J. W.; Hutchinson, J. P.; Zubieta, J. *Inorg. Chim. Acta* **1984**, *91*, L3–L7.

Table IV. UV-Vis Spectral and Other Data for Copper(I) and Dioxygen-Dicopper Complexes[n]

Cu^{I}_2 complexes	Cu^{I}_2 band	Cu_2–O_2 complex	UV-vis bands of the O_2 complexes: 300–400 nm	400–500 nm	500–600 nm	d–d band	Cu···Cu, Å	ν(O–O), cm^{-1}
$[Cu_2(N3)]^{2+}$ (**1a**)	345 (4000)	$[Cu_2(N3)(O_2)]^{2+}$ (**2a**)	365 (15 000)	490 (5250)	600 sh (1200)	>850	3.2[g]	
$[Cu_2(N3OR)]^{2+}$ (**1b**)	375 (3110)	$[Cu_2(N3OR)(O_2)]^{2+}$ (**2b**)	350 (20 000)	485 (1400)	600 sh (880)	875 sh (100)	3.3[g]	
$[Cu_2(N4)]^{2+}$ (**1c**)	350 (3500)[a]	$[Cu_2(N4)(O_2)]^{2+}$ (**2c**)	360 (14 000–16 700)[a]	458 (4500–5300)[a]	550 sh (1200)[a]	775 (200)[a]	3.4[g]	
$[Cu_2(N5)]^{2+}$ (**1d**)	347 (3600)	$[Cu_2(N5)(O_2)]^{2+}$ (**2d**)	360 (21 400)	423 sh (3600)	520 (1200)	>600		
$[Cu_2(XYL\text{-}H)]^{2+}$ (**1e**)	340	$[Cu_2(XYL\text{-}H)(O_2)]^{2+}$ (**2e**)	360[b]	435*[b]				
$[Cu_2(XYL\text{-}F)]^{2+}$ (**1f**)	345 (3250)[b]	$[Cu_2(XYL\text{-}F)(O_2)]^{2+}$ (**2f**)	360 (18 700)[b]	435 (4400)[b]	515 (1300)[b]			
$[Cu_2(UN)]^{2+}$	350 sh	$[Cu_2(UN)(O_2)]^{2+}$	360 (11 000)[m]	520 (1000)[m]	600 sh[m]			
$[Cu_2(XYL\text{-}O\text{-})]^{+}$	318 (9100)[c]	$[Cu_2(XYL\text{-}O\text{-})(O_2)]^{+}$	385 (2900)[c] (PhO → Cu^{II} LMCT)		505 (6000)[c]	787 (700)[c]	3.3[h]	803
	385 (10500)[c]				610 sh (2100)[c]	925 (600)[c]		
$[(tmpa)Cu(RCN)]^{+}$[k]	340 (5600)[d]	$[\{(tmpa)Cu\}_2(O_2)]^{2+}$[k]		440 sh (2000)[d]	525 (11 500)[d]	1035 (160)[d]	4.36[i]	834
					590 (7600)[d]			
$[Cu(HB(3,5\text{-}iPr_2pz)_3]$		$[Cu(HB(3,5\text{-}iPr_2pz)_3]_2(O_2)$	349 (21 000)[l]		551 (800)[l]		3.56	741
deoxy-Hc		oxy-Hc	345 (20 000)[e]	485 (CD)[e,f]	570 (1000)[e]	700 sh (200)[e]	3.6[j]	~750

[a] Reference 2a; variable ε due to dependence on anion and/or presence of MeCN. [b] Reference 5; asterisk indicates unstable intermediate. [c] Reference 11b. [d] Recorded in EtCN solvent; reference 11a. [e] Aqueous media; reference 6a,b. [f] Observed only by circular dichroism. [g] Reference 2b. [h] Reference 31. [i] Reference 11a. [j] Reference 6a,b. [k] tmpa = tris[(2-pyridyl)-methyl]amine. [l] Recorded at −10 °C; ref 36. [m] UN = *N,N,N′,N′*-tetrakis[2-(2-pyridyl)ethyl]-*m*-(aminomethyl)aniline; reference 63. [n] Except where noted, spectra were recorded in dichloromethane at −80 °C. Absorption maxima are given in nm (ε, M^{-1} cm^{-1}).

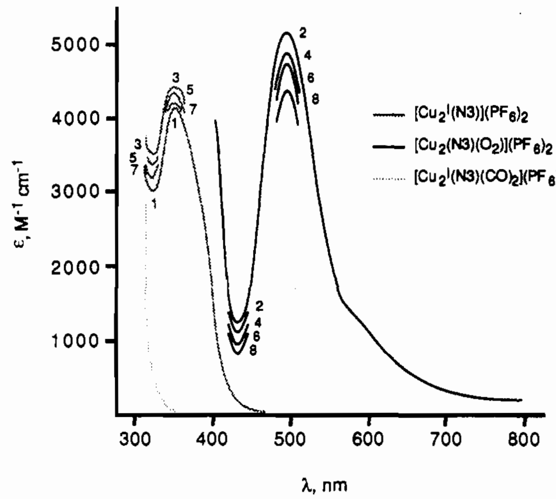

Figure 4. UV–vis spectra demonstrating the reversible dioxygen binding behavior of $[Cu_2(N3)]^{2+}$ (**1a**) in CH_2Cl_2 (vacuum cycling). The bis(carbonyl) complex $[Cu_2(N3)(CO)_2]^{2+}$ (**4a**) (featureless spectrum, ···) is used as a convenient starting material for the experiments, and it is decarbonylated in vacuo at room temperature producing $[Cu_2(N3)]^{2+}$ (**1a**) (spectrum 1, λ_{max} = 345 nm). Oxygenation at −80 °C generates the dioxygen adduct $[Cu_2(N3)(O_2)]^{2+}$ (**2a**) (spectrum 2, λ_{max} = 490, 365 nm, peak not shown). Application of a vacuum to the solution and rapid warming to 100 °C removes the bound dioxygen ligand, regenerating **1a**. The cycling can be repeated several times as shown.

plementary material, respectively.

Reversible Binding of Dioxygen. Vacuum Cycling. Metal complexes that bind dioxygen reversibly are defined as compounds that, upon interaction with O_2, form discrete $M_n(O_2)$ species, with the O–O bond unbroken and for which the O_2 can be liberated by varying the external conditions.[32,33] The 2:1 Cu:O_2 stoichiometry of dioxygen binding to dicopper(I) complexes $[Cu_2(L)]^{2+}$ (**1**) strongly suggests that the O–O bond is intact in O_2-adducts **2**. The reversibility of dioxygen binding to solutions of **1** (or **3**) is indicated by the ability to oxygenate these complexes and deoxygenate the resulting O_2 complexes (**2**) through the application of heat and a vacuum while recovering both the precursors $[Cu_2(Nn)]^{2+}$ (**1**) and dioxygen in good yield. We have been able to identify both qualitatively and quantitatively the gas removed.

An experiment illustrating repetitive cycling between deoxy and oxy forms using the N3 ligand complexes is shown in Figure 4. Here, as followed spectrophotometrically, the application of vacuum/Ar-purging of room-temperature solutions of $[Cu_2(N3)(CO)_2]^{2+}$ (**4a**) provides $[Cu_2(N3)]^{2+}$ (**1a**), spectrum 1. Cooling to −80 °C and exposure to O_2 results in the rapid formation of $[Cu_2(N3)(O_2)]^{2+}$ (**2a**), with its characteristic spectrum 2, as monitored by the 490-nm absorption. When this solution is subjected to vacuum and rapidly and briefly (1–5 s) heated to 100 °C, the intense brown color is lost. At this point, the lost solvent is replaced, the solution is again cooled to −80 °C, and the spectrum recorded (spectrum 3, Figure 4) indicates the regeneration of $[Cu_2(N3)]^{2+}$ (**1a**). Reoxygenation of this solution affords $[Cu_2(N3)(O_2)]^{2+}$ (**2a**), spectrum 4. As shown, four oxygenation/deoxygenation cycles can be carried out; the decomposition is minimal as indicated by the relatively small loss in absorbance of the 490-nm band of **2a**.

Vacuum-cycling experiments analogous to that shown for the N3 ligand complexes (Figure 4) were also carried out with N3OR- and N5-containing species. Spectrophotometric illustrations of these experiments are presented in the supplementary material.

Identification and Quantitation of O_2 Bound in Complexes $[Cu_2(Nn)(O_2)]^{2+}$ (2). We previously described the qualitative identification of O_2, when removed from solutions of $[Cu_2(N4)(O_2)]^{2+}$ (**2c**).[2a] The same procedure was applied here for

---

[32] Niederhoffer, E. C.; Timmons, J. H.; Martell, A. E. *Chem. Rev.* **1984**, *84*, 137.

[33] Karlin, K. D.; Gultneh, Y. *J. Chem. Educ.* **1985**, *62*, 983–990.

O_2 complexes with ligands N3, N3OR, and N5.[11b,14] Excess O_2 is first removed from **2c** by application of a vacuum to the dichloromethane solutions at −80 °C. Then, the vacuum-cycling experiment is carried out in such a way so as to trap out (−196 °C) the liberated gas and solvent, when the solutions of $[Cu_2(L)(O_2)]^{2+}$ (**2**) are heated and exposed to a static vacuum. In this way, O_2 is identified by releasing (warming) the trapped gas and allowing it to pass through a degassed colorless alkaline pyrogallol (1,2,3-trihydroxybenzene) test solution, which turns brown when exposed to dioxygen.

As briefly described in footnote 50 of ref 2a, we have also been able to indirectly quantitate the amount of dioxygen bound in complexes $[Cu_2(Nn)(O_2)]^{2+}$ (**2**), using a gravimetric method we have developed. Here, we start by removing the dioxygen from cold solutions of $[Cu_2(Nn)(O_2)]^{2+}$ (**2**) by the same procedure described above, trapping it at −196 °C. Then, we allow this trapped gas to warm up in a closed system, exposing it to solutions of the dicopper(I) complex $[Cu_2(QPY2)(CH_3CN)_2](PF_6)_2$ (**6**), which contains a 5-OH-substituted *m*-XYL ligand, as shown below. In CH_2Cl_2 as solvent, **6** is known to react with O_2 in a highly reproducible manner having a 4:1 Cu:O_2 stoichiometry (manometry), producing a compound with the composition $[Cu_2(QPY2-2H+O)Cl_2](PF_6)_2$ (**7**).[15] The exact structure of the product is unknown at present, but it is believed to contain a hydroxylated xylyl ring, since such a product has been obtained and structurally characterized when the reaction of **6** with O_2 is subjected to somewhat similar conditions.[15] Complex **7** is insoluble in CH_2Cl_2 and readily and completely precipitates as a stable purple solid providing a straightforward means of determining how much O_2 is present. Thus, the trapped gas obtained from a known amount of dioxygen complex **2** was exposed to an excess of **6** in a closed system, and the solution was filtered under argon. From the weight of **7** obtained, the amount of O_2 removed from solutions of dioxygen complexes $[Cu_2(Nn)(O_2)]^{2+}$ (**2**) could be back-calculated. Experiments performed in this manner for $[Cu_2(N3OR)(O_2)]^{2+}$ (**2b**) and $[Cu_2(N4)(O_2)]^{2+}$ (**2c**) provided the result that 83% of the O_2 expected from **2b** was recovered by this trapping method; as previously reported,[2b] 82% of that expected from a solution of **2c** was obtained (see Experimental Section). Thus, these results also corroborate the manometrically determined stoichiometry of the reaction of O_2 with dicopper(I) complexes $[Cu_2(Nn)]^{2+}$ (**1**), e.g. 2:1 Cu:O_2, but by means of determining how much O_2 can be removed from complexes $[Cu_2(NnL)(O_2)]^{2+}$ (**2**).

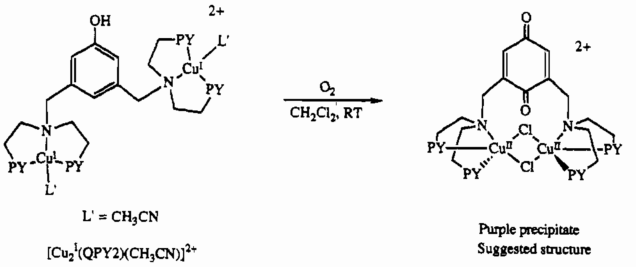

Reversible Binding of O_2 and CO and Displacement of O_2 by CO. Carbonyl Cycling. Another indication that solutions of $[Cu_2(Nn)]^{2+}$ (**1**) bind O_2 reversibly comes from the observation that a small molecule such as CO can displace O_2, with further evidence that O_2 is released. As was observed for the N4 ligand complexes,[2a] the binding of CO to the three-coordinate dicopper(I) complexes **1** is stronger than that of O_2. At temperatures low enough to stabilize dioxygen adducts $[Cu_2(Nn)(O_2)]^{2+}$ (**2**), dioxygen will *not* react with the bis(carbonyl) adducts $[Cu_2(Nn)(CO_2)]^{2+}$ (**4**). As already indicated, CO readily binds to three-coordinate Cu(I) moieties in **1**, and this is a reversible process. Thus, the reversible CO and O_2 binding to **1** and the CO displacement of O_2 make for carbonyl cycling, which can be followed spectrophotometrically.

This behavior is shown for the N3OR ligand complexes in Figure 5, where $[Cu_2(N3OR)]^{2+}$ (**1b**) reacts with O_2 (−80 °C in CH_2Cl_2) to give $[Cu_2(N3OR)(O_2)]^{2+}$ (**2b**), from which the O_2 ligand is displaced by CO to give $[Cu_2(N3OR)(CO_2)]^{2+}$ (**4b**). Such experiments are conducted in a spectrophotometric cell, with solution concentrations of the order 10^{-4}–10^{-5} M. The displacement of O_2 does not occur readily at −80 °C but is effected by saturation of the solution of **2b** with carbon monoxide, followed by warming for brief periods (i.e., exposure to room temperature for 30 s) until the solution had decolorized. Following these procedures, **1b** (spectrum 1) is oxygenated to give **2b** (spectrum 2, 350-nm band shown), and this is reacted with CO to give **4b**, with featureless spectrum 3. Warming to room temperature and application of a vacuum removes the bound CO, regenerating $[Cu_2(N3OR)]^{2+}$ (**1b**). As shown, four deoxy → oxy → bis(carbonyl) adduct cycles can be carried out without a severe amount of decomposition. Carbonyl-cycling experiments were also carried out with the complexes using the N3 and N5 ligands, and similar behavior is observed. Figures presenting these latter experiments are given in the supplementary material.

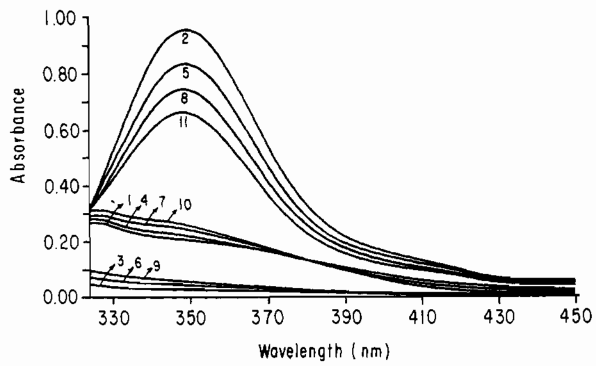

Figure 5. UV–vis spectra demonstrating the reversible O_2 and CO binding behavior of the tricoordinate complex $[Cu_2(N3OR)]^{2+}$ (**1b**) in CH_2Cl_2 (carbonyl cycling). A solution of $[Cu_2(N3OR)]^{2+}$ (**1b**) (4.97×10^{-5} M, spectrum 1) is oxygenated at −80 °C producing $[Cu_2(N3OR)(O_2)]^{2+}$ (**2b**) (spectrum 2, $\lambda_{max} = 350$ nm). This solution is then saturated with CO, and with some warming, the O_2 ligand is displaced and the bis(carbonyl) adduct, $[Cu_2(N3OR)(CO)_2]^{2+}$, is generated (featureless spectrum 3). This solution is then decarbonylated in vacuo at room temperature to give back $[Cu_2(N3OR)]^{2+}$ (**1b**) (spectrum 4). The process can be repeated, and four cycles are shown. The 485, 600, and 875 (sh) nm bands of $[Cu_2(N3OR)(O_2)]^{2+}$ (**2b**) are not shown.

As found for the vacuum-cycling experiments, dioxygen is seen to be evolved from solutions of $[Cu_2(N3OR)(O_2)]^{2+}$ (**2b**) as well as the other dioxygen complexes $[Cu_2(Nn)(O_2)]^{2+}$ (**2**), when they are subjected to CO as described above. A dichloromethane solution of $[Cu_2(N3OR)(O_2)]^{2+}$ (**2b**) can be purged of any excess O_2 in the solvent, by either (a) alternating vacuum/purge cycles under argon or (b) flushing the solution with Ar or CO. When such a solution of **2b** is bubbled continuously with CO at −80 °C and the gas that passes through the solution is then bubbled through a clear and colorless pyrogallol test solution, no change occurs since CO does not displace O_2 from **2b** under these conditions. However, when the solution of **2b** is warmed up with shaking while bubbling with carbon monoxide, the test solution turns brown, indicating dioxygen has been released.

As before[2a] the possibility that CO_2 might be produced by reaction of CO with dioxygen complexes $[Cu_2(Nn)(O_2)]^{2+}$ (**2**, L = N3, N3OR, N5) was checked by passing the gas stream through an aqueous $Ba(OH)_2$ solution. No detectable $BaCO_3$ was observed, indicating that CO_2 is not produced in this reaction. There is a recent report that a carbonato complex is produced when CO is reacted with a species derived from the interaction of O_2 with $[Cu_2(N\text{-}N)_2I_2]$ (N-N = 2,2′-bipyridine or 1,10-phenanthroline) in the presence of 2-methylimidazole.[34]

Properties of $[Cu_2(L)(O_2)]^{2+}$ (2) Complexes and Proposed Structure. On the basis of physical and chemical properties (vide infra) of copper–dioxygen species $[Cu_2(L)(O_2)]^{2+}$ (**2**), we suggest they are best formulated as peroxodicopper(II) complexes and

---

[34] Bhaduri, S.; Sapre, N. Y.; Basu, A. *J. Chem. Soc., Chem. Commun.* **1986**, 197–198.

propose that they possess the μ-η^2:η^2-peroxo-bridging structure shown as

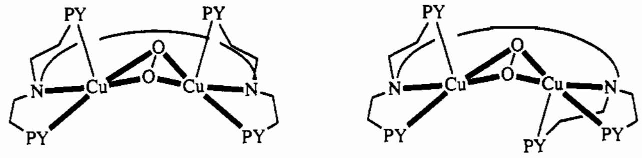

Proposed Structures for $[Cu_2(L)(O_2)]^{2+}$ (2) Complexes

The indicated structures are suggested for complexes **2**, where L can either be N*n* (N3, N3OR, N4, N5) or the closely related XYL (*m*-xylyl or substituted ligand XYL-X) dinucleating ligands (Figure 1). We propose that each Cu(II) ion is found in a roughly square-based pyramidal environment with one amine nitrogen, one pyridine, and the two oxygen atoms of the peroxo ligand occupying a basal plane, with the other pyridine group axially ligated. One structure shown possesses a plane of symmetry, passing through the peroxo O–O bond and dividing the two halves of the molecule; here the axial pyridine ligands would both be on the same side of the copper basal planes. Molecular models suggest that this structure may be additionally stabilized by a stacking of the axial pyridine groups, as we have seen in another dinuclear complex containing the PY2 unit and where Cu···Cu = 3.3 Å.[30b] Another configuration which cannot be distinguished from data currently in hand has the axial pyridine ligands on opposite sides of the Cu_2O_2 moiety, as shown.

The bent butterflylike μ-η^2:η^2 structure shown is suggested to accommodate reasonable Cu–O bond lengths along with the Cu···Cu distances observed from EXAFS (extended X-ray absorption fine structure) spectroscopic analyses performed on solutions of **2a–c**; these provided values of 3.2 Å for $[Cu_2(N3)(O_2)]^{2+}$ (**2a**) ranging to 3.4 Å for $[Cu_2(N4)(O_2)]^{2+}$ (**2c**).[2b] While we stated that a cis-μ-1,2-peroxo-bridging structure should also be considered for **2a–c**, the detailed outer-shell multiple scattering analysis of the EXAFS spectroscopic data led to a better fitting for the μ-η^2:η^2 configuration, primarily since it would possess only one closely bonded (i.e., in-plane) pyridine ring.[2b] The proposal was novel and speculative at the time, since such structures are rare for metal–O_2 complexes (a peroxo-bridged divanadium complex with a bent side-on O_2^{2-} structure is known[35b]),[35] and this mode of peroxo coordination had not previously been considered for copper ions. However, a significant breakthrough in this field was made recently through a contribution by Kitajima and co-workers,[36] who structurally characterized $[Cu(HB(3,5\text{-}iPr_2pz)_3]_2(O_2)$, possessing a *planar* μ-η^2:η^2-peroxo structure, thus confirming the viability of this type of coordination and raising it as a strong candidate for the structure of oxyhemocyanin (see further discussion below).[37,38]

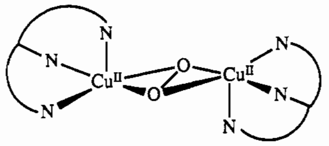

$\{Cu[HB(3,5\text{-}iPr_2pz)_3]\}_2(O_2)$

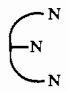

= hydrotris(3,5-diisopropyl-pyrazolyl)borate anion

Cu...Cu = 3.56 Å   O-O = 1.41 Å

Distorted square pyramidal

A number of other physical properties and observations concerning complexes $[Cu_2(Nn)(O_2)]^{2+}$ (**2**) are of interest, and while they do not necessarily directly point to the μ-η^2:η^2 structure, they are consistent with this proposal.

Complex Formulation. The formulation of the complexes as peroxodicopper(II) complexes $[Cu^{II}_2(N4)(O_2^{2-})]^{2+}$ (**2**) follows arguments previously made for $[Cu_2(N4)(O_2)]^{2+}$ (**2c**),[2a] which were based on (a) the presence of d–d bands, (b) identification of Cu(II) from X-ray absorption studies, and (c) the observed Cu:O_2 = 2:1 dioxygen binding stoichiometry, consistent with the usual notions that O_2 binding to metals is accompanied by a fair degree of electron transfer.[35a] All of the $[Cu_2(Nn)(O_2)]^{2+}$ (**2**) complexes possess an absorption band in the visible region (>600 nm, Table IV), which can be assigned with confidence as a d–d absorption due to their low energy and intensity. This confirms that the copper is present as Cu(II) with its $3d^9$ electronic configuration, since a filled-shell $3d^{10}$ Cu(I) ion would not possess any ligand field absorption bands. The evidence from X-ray absorption studies comes from the fact that Cu(I) complexes are known to possess a prominent Cu K absorption edge feature which is not present in Cu(II) compounds. It was also found that oxygenation of dicopper(I) complexes **1a–c** resulted in the loss of this characteristic, with a resulting shift to values to those typical of well-characterized dicopper(II) compounds.[2b]

The O–O stretching vibrational frequency is another property useful in the characterization of bound dioxygen species. This is usually obtained by IR or resonance Raman spectroscopies, and we have been previously capable in characterizing two other classes of $\{Cu_2\text{–}O_2\}^{n+}$ complexes using the latter technique.[39] Unfortunately, we have not been successful in obtaining such data for complexes $[Cu_2(Nn)(O_2)]^{2+}$ (**2**), as initial attempts where thwarted, apparently by laser light initiated photodecomposition.[40] It is noteworthy that Kitajima and co-workers have successfully obtained such data for $[Cu(HB(3,5\text{-}iPr_2pz)_3]_2(O_2)$, with $\nu_{O\text{–}O}$ = 741 cm^{-1}.[36] This is at the low end of the range typically found for metal peroxides (O_2^{2-}),[35,42] consistent with the bonding expected for this μ-η^2:η^2-peroxo structure,[37,41] and it also closely coincides with the values observed for oxyhemocyanins.[6,43]

NMR and Magnetic Properties. The magnetic properties of the dioxygen complex species $[Cu_2(Nn)(O_2)]^{2+}$ (**2**) are of interest, in terms of the structure we have proposed and the general role of an O_2^{2-} ligand in mediating electron/magnetic interactions between Cu(II) ions. As previously observed,[2a] $[Cu_2(N4)(O_2)]^{2+}$ (**2c**) is EPR silent, and measurements carried out on frozen solutions of the other complexes $[Cu_2(Nn)(O_2)]^{2+}$ (**2a–d**) indicate the same behavior. When handled very carefully, no peaks at all are observed for EPR spectra taken at 77 K in dichloromethane or CH_2Cl_2/toluene glasses. Occasionally, a broad absorption is seen in the g = 2.1 region, but comparisons with monomeric Cu(II) standards indicate that such signals represent only a few percent of the copper present. In addition, when solutions of **2a–d** are allowed to decompose by warming briefly above −80 °C, these signals increase in intensity, suggesting they are due to impurities.

While the EPR silence of these peroxodicopper(II) complexes is consistent with the presence of antiferromagnetically coupled copper(II) centers, better evidence is provided through NMR

---

(35) (a) Gubelmann, M. H.; Williams, A. F. *Struct. Bonding (Berlin)* **1983**, *55*, 1. (b) A divanadium peroxo complex with μ-η^2:η^2 structure is known: Schwendt, P.; Joniakova, D. *Polyhedron* **1984**, *3*, 287–290.

(36) (a) Kitajima, N.; Fujisawa, K.; Moro-oka, Y.; Toriumi, K. *J. Am. Chem. Soc.* **1989**, *111*, 8975–8976. (b) Kitajima, N.; Koda, T.; Hashimoto, S.; Kitagawa, T.; Moro-oka, Y. *J. Am. Chem. Soc.* **1991**, *113*, 5664–5671. (c) Kitajima, N.; Fujisawa, K.; Fujimoto, C.; Moro-oka, Y.; Hashimoto, S.; Kitagawa, T.; Toriumi, K.; Tatsumi, K.; Nakamura, A. *J. Am. Chem. Soc.* **1992**, *114*, 1277–1291.

(37) Ross, P. K.; Solomon, E. I. *J. Am. Chem. Soc.* **1991**, *113*, 3246–3259.

(38) Karlin, K. D.; Tyeklár, Z.; Farooq, A.; Jacobson, R. R.; Sinn, E.; Lee, D. W.; Bradshaw, J. E.; Wilson, L. J. *Inorg. Chim. Acta* **1991**, *182*, 1–3.

(39) (a) Pate, J. E.; Cruse, R. W.; Karlin, K. D.; Solomon, E. I. *J. Am. Chem. Soc.* **1987**, *109*, 2624–2630. (b) Baldwin, M. J.; Ross, P. K.; Pate, J. E.; Tyeklár, Z.; Karlin, K. D.; Solomon, E. I. *J. Am. Chem. Soc.* **1991**, *113*, 8671–8679.

(40) Solomon, E. I., Stanford University, private communication.

(41) A recent theoretical study carried out on the bonding involved in the μ-η^2:η^2-peroxo–dicopper(II) structure indicates that the peroxide σ^* orbital acts as a π-acceptor orbital, offering an explanation for the low O–O stretching frequency observed. See ref 37.

(42) (a) Barraclough, C. S.; Lawrance, G. A.; Lay, P. A. *Inorg. Chem.* **1978**, *17*, 3317–3322. (b) Griffith, W. P.; Wickins, T. D. *J. Chem. Soc. A* **1968**, 397–400.

(43) (a) Larrabee, J. A.; Spiro, T. G. *J. Am. Chem. Soc.* **1980**, *102*, 4217–4223. (b) Freedman, T. B.; Loehr, J. S.; Loehr, T. M. *Ibid.* **1976**, *98*, 2809–2815.

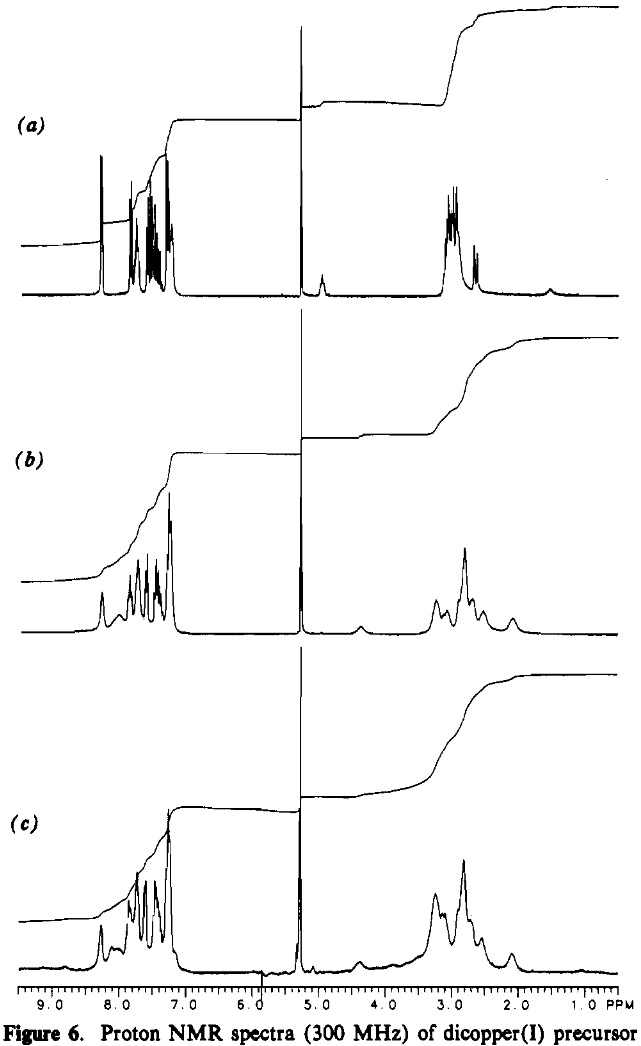

Figure 6. Proton NMR spectra (300 MHz) of dicopper(I) precursor complex $[Cu_2(N3OR)]^{2+}$ (**1b**) at room temperature (CD_2Cl_2) (spectrum a) and at −80 °C (spectrum b) and the dioxygen complex itself, $[Cu_2(N3OR)(O_2)]^{2+}$ (**2b**). The NMR sample of **2b** was prepared by addition of O_2 to **1b** at −80 °C, followed by vacuum/Ar-purge cycles to remove excess O_2. See the text for further discussion.

studies and direct magnetic measurements. We find that solutions of $[Cu_2(Nn)(O_2)]^{2+}$ (**2a–d**) at −80 °C exhibit ^1H NMR spectra essentially unchanged from those of the precursor complexes $[Cu_2(Nn)]^{2+}$ (**1a–d**), and representative spectra are shown for **1b** and **2b** in Figure 6. Room-temperature spectra of **1a–d** are sharp, as expected for diamagnetic Cu(I) compounds, having chemical shifts very close to those observed for the free ligands, and reduction in temperature to −80 °C causes some broadening. However, oxygenation gives essentially the identical spectrum seen for the low-temperature dicopper(I) complex spectrum, and the minor loss in intensity observed (ca. 10–30%) is probably due to the presence of small amounts of a paramagnetic impurity.

Susceptibility experiments represent the best means by which to determine the magnetic properties of these dicopper(II) species. While we performed numerous single-temperature (−80 °C) Evans method susceptibility measurements on $[Cu_2(Nn)(O_2)]^{2+}$ (**2**),[44] this approach was thwarted by the variable (although small) amounts of impurities present, resulting in rather inconsistent results.[45] However, we recently carried out variable-temperature (80–160 K) Faraday susceptibility measurements on $[Cu_2(N4)(O_2)]^{2+}$ (**2c**) in dichloromethane solution.[38] The findings are consistent with the EPR and NMR results, suggesting that **2c** is essentially diamagnetic; a conservative lower limit for $-2J$ can be assigned as $-2J \geq 600$ cm^{-1} based on $H_{ex} = -2JS_1{\cdot}S_2$.

Thus, the peroxo ligand in $[Cu_2(Nn)(O_2)]^{2+}$ (**2**) is capable of mediating very strong antiferromagnetic coupling, where it is the only bridging ligand present. These findings are in agreement with the results reported by Kitajima and co-workers for $[Cu(HB(3,5\text{-}iPr_2pz)_3]_2(O_2)$, which was also reported to be diamagnetic based only upon EPR (i.e., silent) and NMR criteria, where the complex showed "normal" behavior and $\mu_B = 0$ (Evans method) at −10 °C in toluene.[36] We have also obtained both solution and solid-state magnetic susceptibility data[38] for the other structurally characterized peroxodicopper(II) complex, $[\{(tmpa)Cu\}_2(O_2)]^{2+}$ (tmpa = tris[(2-pyridyl)methyl]amine), containing a single trans-μ-1,2-peroxo ligand (Cu···Cu = 4.36 Å).[1,11a] The data also are indicative of an essentially diamagnetic system, with $-2J$ clearly greater than 600–700 cm^{-1}.[38] Thus, in at least two bridging modes, i.e., μ-η^2:η^2 or trans-μ-1,2 the peroxo (O_2^{2-}) ligand is capable of mediating strong magnetic coupling between copper(II) ions.

UV–Vis Spectroscopic Comparisons. As discussed above, $[Cu_2(Nn)(O_2)]^{2+}$ (**2a–d**) are characterized by strong and multiple absorptions in the UV–vis region (Figures 3–5; Table IV). In particular, the very intense absorption occurring at 350–365 nm with ϵ ranging from 14 000 to 21 400 M^{-1} cm^{-1} is striking. These spectra qualitatively resemble that observed for oxyhemocyanin (Table IV). From extensive spectroscopic analyses, Solomon and co-workers have assigned the strong bands in oxy-Hc as peroxo-to-Cu(II) ligand-to-metal charge-transfer (LMCT) absorptions. Since a maximum of two charge-transfer transitions can be observed for a terminally bound peroxide–copper monomer geometry (referred to as peroxide π^*_σ and π^*_v to Cu^{II}), the presence of more than two such absorptions for oxy-Hc and the $[Cu_2(Nn)(O_2)]^{2+}$ (**2a–d**) complexes also indicates that the peroxo ligand bridges the two Cu(II) ions.[6a,b,46]

While the UV–vis spectra of the different $[Cu_2(Nn)(O_2)]^{2+}$ (**2a–d**) structures all exhibit similar patterns (Table IV), there are large variations in the position and intensities of the 400–500 and 500–600-nm CT absorptions. We suggest that these differences can be ascribed to the effect of the alkane chain linker connecting the two PY2 tridentate donor units. Examination of molecular models indicates that ligand constraints caused by the length of the linker (i.e. n in Nn) affects the relative flattening of the μ-η^2:η^2-peroxo moiety, such that if a longer linker than is found in the N5 ligand were used, a planar structure might be allowed. The trend observed for EXAFS spectroscopically derived Cu···Cu distances is consistent with this argument (Table IV). Note that CT transitions would be expected to be greatly affected by subtleties of local environment, polarity, etc.

There is one major difference in the UV–vis spectra of oxy-Hc and $[Cu_2(Nn)(O_2)]^{2+}$ (**2a–d**), the absorption found in the 400–500-nm region. This is found at variable positions and intensity for **2a–d** but is only seen by circular dichroism (CD) (for mulluscan Hc's) in the protein (Table IV). The group theoretical arguments by Solomon and co-workers[6a,b] show that this LMCT transition should be CD allowed and absorption disallowed for a high-symmetry $Cu^{II}{}_2O_2{}^{2-}$ structure (e.g. cis-μ-1,2-peroxo or μ-η^2:η^2-peroxo[37]). However, lowering the symmetry by tilting the coordinated peroxo group out of plane should "allow" absorption intensity into this band; this indeed occurs in arthropod oxy-Hc's compared to those of molluscs, and one sees an increase in the absorption intensity in the region of 480 nm for the arthropods.[47] We suggest that similar reasoning may be applied to the bent μ-η^2:η^2-peroxo structures we propose for $[Cu_2(Nn)(O_2)]^{2+}$ (**2a–d**) and that large absorptions seen in the 423–490-nm region of **2a–d** may originate from the nonplanarity in these systems, which is a probable consequence of ligand constraints (vide supra).

It is also important to note the similarity of UV–vis spectra found for $[Cu_2(Nn)(O_2)]^{2+}$ (**2a–d**) and $[Cu_2(XYL\text{-}X)(O_2)]^{2+}$

---

[44] (a) Evans, D. F. *J. Chem. Soc.* **1959**, 2003. (b) Live, D. H.; Chan, S. I. *Anal. Chem.* **1970**, *42*, 79.

[45] Karlin, K. D.; Tyeklár, Z.; Haka, M. S. Unpublished results.

[46] Eickman, N. C.; Himmelwright, R. S.; Solomon, E. I. *Proc. Natl. Acad. Sci. U.S.A.* **1979**, *76*, 2094–2098.

[47] Himmelwright, R. S.; Eickman, N. C.; LuBien, C. D.; Solomon, E. I. *J. Am. Chem. Soc.* **1980**, *102*, 5378–5388.

Table V. Electrochemical Data for $[Cu^{I}_2(L)]^{2+}$ (**1**) and $[Cu_2(L)(O_2)]^{2+}$ (**2**) Complexes

complex[a]	$E_{1/2}$,[b,c] V (ΔE_p, mV) DMF	$E_{1/2}$,[b,c] V (ΔE_p, mV) CH_2Cl_2	E_{pc} of $[Cu_2(L)(O_2)]^{2+}$ (**2**),[d] V CH_2Cl_2
$[Cu^{I}_2(N3)]^{2+}$ (**1a**)	0.27 (260)	0.75 (200)	−1.1
$[Cu^{I}_2(N3OR)]^{2+}$ (**1b**)	0.32 (120)	0.90 (310)	−1.2
$[Cu^{I}_2(N4)]^{2+}$ (**1c**)	0.29 (220)	0.77 (170)	−0.9
$[Cu^{I}_2(N5)]^{2+}$ (**1d**)	0.38 (260)	0.75 (330)	*e*
$[Cu^{I}_2(XYL\text{-}H)]^{2+}$ (**1e**)	0.31 (160)[e,f]	*g*	*g*
$[Cu^{I}(MePY2)]^{+}$	0.23 (90)[h]	*g*	*g*

[a] Coulometric experiments show $2e^-$ current passed per molecule. [b] Measurements are reported with respect to GCE as working electrode at a scan rate of 100 mV s^{-1}. [c] Potentials are reported vs Ag/AgCl; Fc/Fc^+ values are given in the Experimental Section. [d] CV's were taken at −80 °C. [e] Previously[4b] incorrectly reported as 0.16 V. [f] Previously measured in MeOH solvent as 0.33 V Ag(s).[51] [g] Measurements were not made. [h] Reference 48a.

(**2e–f**, X = H or F; Figure 1, diagram above, and Table IV). The XYL-X ligand complexes are very similar to those of N*n*, having five carbons connecting the two tertiary amine nitrogen atoms of the PY2 units. As mentioned in the Introduction, the reaction of $[Cu_2(XYL\text{-}H)]^{2+}$ (**1e**) with O_2 represents a very good model system for copper monooxygenases,[1,4a] as a consequence of the ensuing hydroxylation of the ligand; substantial evidence exists for the intermediacy of $[Cu_2(XYL\text{-}H)(O_2)]^{2+}$ (**2e**) in this reaction.[1,9,10] The similarity of spectra of **2a–d** with **2e–f** has been used as further evidence for the existence of **2e** (X = H).[1,5] Note that there is in fact a much greater likeness of UV–vis spectra of $[Cu_2(N5)(O_2)]^{2+}$ (**2d**) with $[Cu_2(XYL\text{-}X)(O_2)]^{2+}$ (**2e–f**) than with the other complexes **2a–c**, again pointing to the importance of differences caused by the varied linkers (*n*) in these N*n* dinucleating ligands.

Intra- vs Intermolecular O_2 Binding. In the discussions above, we have assumed that the oxygenation of dicopper(I) precursors $[Cu_2(Nn)]^{2+}$ (**1**) leads to discrete dinuclear peroxodicopper(II) complexes $[Cu_2(Nn)(O_2)]^{2+}$ (**2**), as a result of the binding of O_2 by an *intra*molecular process. While we cannot unambiguously rule out the possibility of cluster formation, i.e. $\{[Cu_2(Nn)(O_2)]^{2+}\}_n$, there are several lines of evidence suggesting that this is *not* the case. (i) The product peroxodicopper(II) complexes are very soluble in the −80 °C dichloromethane solutions; polynuclear cationic complexes would be less likely to have this property. (ii) The reactions of precursors $[Cu_2(L)(O_2)]^{2+}$ (**1**) with O_2 are very fast, even at −80 °C. The kinetic study carried out on the oxygenation of $[Cu_2(XYL\text{-}H)]^{2+}$ (**1e**) confirms this (k_{on} = 533 M^{-1} s^{-1} at −80 °C) and also indicates that the reaction is strictly first order with respect to **1e**,[9] i.e., intramolecular. (iii) The reactions of $[Cu_2(Nn)]^{2+}$ (**1**) with O_2 are also qualitatively very fast, and preliminary kinetic studies also suggest a first-order dependence on **1**.[48a] These results can be compared to the slow oxygenation rates (e.g. minutes to hours at −80 °C) observed for monomeric analogues $[Cu^{I}(RPY2)]^{+}$ (R = Me, $PhCH_2$, Ph), which also form

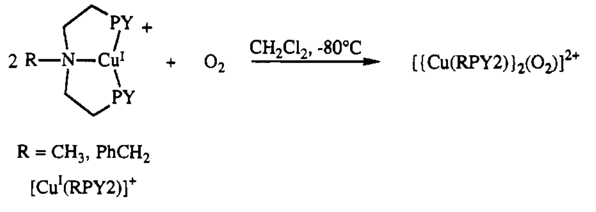

R = CH_3, $PhCH_2$

$[Cu^{I}(RPY2)]^{+}$

dioxygen complexes $\{[Cu(RPY2)](O_2)\}^{2+}$ and have UV–vis spectra very similar to that of $[Cu_2(Nn)(O_2)]^{2+}$ (**2**).[48] (iv) The spectral dependence upon *n* observed for $[Cu_2(Nn)(O_2)]^{2+}$ (**2**) also argues for *intra*molecular association of O_2, since *inter*molecular interactions are unlikely to be influenced by the alkane chain linker length. Spectra of $\{[Cu(RPY2)](O_2)\}^{2+}$ more closely resemble $[Cu_2(N5)(O_2)]^{2+}$ (**2d**), where the evidence suggests that complexes with N5 are probably the least constrained.

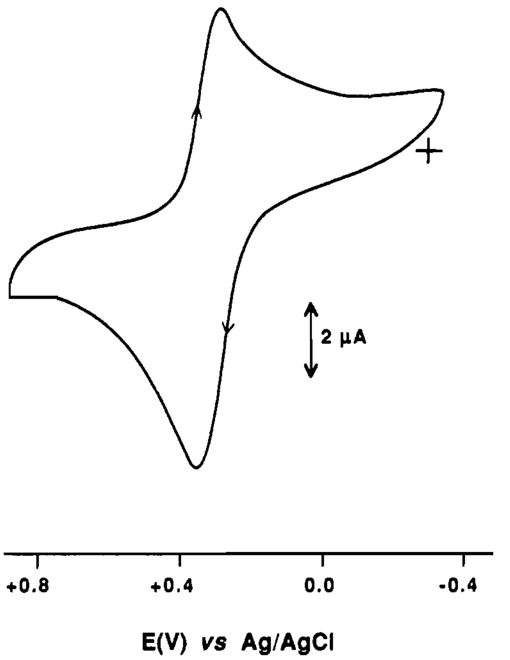

Figure 7. Cyclic voltammogram (CV) of $[Cu_2(N3)]^{2+}$ (**1a**) in dimethylformamide solution at room temperature, using a GCE working electrode.

Electrochemistry. The electrochemical behavior of dicopper(I) complexes $[Cu_2(L)]^{2+}$ (**1a–e**) and the peroxodicopper(II) species $[Cu_2(Nn)(O_2)]^{2+}$ (**2a–c**) was examined using cyclic voltammetry (CV), and the results are given in Table V. In dimethylformamide (DMF), **1a–e** displayed a single quasireversible redox process over the potential interval −1.0 to +1.5 V versus Ag/AgCl. The peak-to-peak current ratios (i_{pa}/i_{pc}) were very close to unity over a scan rate range 100–1000 mV/s, and a typical CV scan is given for $[Cu_2(N3)]^{2+}$ (**1a**) in Figure 7. Analysis of the peak current function $i_p/v^{1/2}C$ (v = scan rate, C = concentration) corresponded to a 2-electron process per dinuclear complex, when compared to a known mononuclear standard ($[Cu(MePY2)](ClO_4)_2$,[48a] and constant-potential electrolysis (at +0.8 V) of solutions of **1** gave *n* values of 1.9–2.2; these experiments were accompanied by a color change from light yellow to blue-green. The CV of a coulometrically oxidized solution gave the exact complement of that of the original solution at the same scan rate. These observations all demonstrate an effective reversibility via an overall 2-electron-transfer reaction:

$$\underset{\text{1a-e}}{[Cu_2^{I}(L)]^{2+}} + 2e^- \rightleftharpoons [Cu_2^{II}(L)]^{4+}$$

From the data given in Table V, it is evident that there is little if any dependence of the $E_{1/2}$ value upon the length of the methylene chain linking separate redox-active centers in these dinuclear complexes. Moreover, there is no evidence for distinct oxidative processes occurring for the two Cu ion centers, as might be expected for such closely linked centers. As revealed by differential pulse voltammetric measurements, a recent study of bis(cyclam)dinickel and -dicopper complexes possessing variable methylene or xylyl linkers indicates how electrostatic effects and metal-metal distance (as modified by linker length) can influence the occurrence or extent of separation of the two metal-centered redox processes.[49] However, the cyclic voltammetric experiments here, even when exploring scan-rate dependencies,[50] offer no indication of other than essentially independent processes occurring

---

(48) (a) Karlin, K. D. and co-workers, unpublished results. (b) Cruse, R. W. Ph.D. Thesis, State University of New York at Albany, 1986.

(49) Ciampolini, M.; Fabbrizzi, L.; Perotti, A.; Poggi, A.; Seghi, B.; Zanobini, F. *Inorg. Chem.* **1987**, *26*, 3527–3533.

(50) A recent study indicates that CV scan rate changes may reveal two one-electron components of a single-step two-electron-transfer process: Pierce, D. T.; Geiger, W. E. *J. Am. Chem. Soc.* **1989**, *111*, 7636–7638.

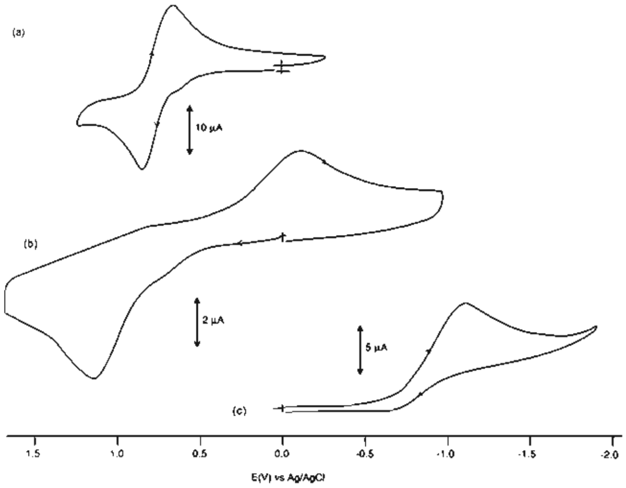

Figure 8. Cyclic voltammograms of $[Cu_2(N3)]^{2+}$ (**1a**) and O_2 complex in dichloromethane solution (GCE working electrode): (a) room-temperature CV; (b) same solution at −80 °C; (c) after formation of $[Cu_2(N3)(O_2)]^{2+}$ (**2a**) by bubbling with O_2 followed by purging/bubbling with Ar to remove excess dioxygen.

at both copper ions of the dinuclear complexes studied here. A similar observation was made by Sorrell and co-workers, who examined **1e** in methanol solvent and compared its behavior to a closely related dicopper(I) complex containing pyrazole rather than pyridine donor ligands.[51] A small redox potential shift may be observed for the monomeric *N*-methyl-substituted PY2-containing complex $[Cu^I(MePY2)]^+$, where $E_{1/2}$ is 0.23 V vs Ag/AgCl (Table V), ~0.05 V more negative than observed for these dinuclear complexes **1a–e**. The larger values in **1a–e** may arise from the effect of a nearby positively charged center in making the oxidation of one of the Cu(I) ions more difficult.

The redox potentials of **1a–e** are considerably more positive in dichloromethane solvent than in DMF, more so than would be expected from the differences in dielectric constants of these two solvent media.[52] The explanation for this undoubtedly lies in the coordinating ability of DMF as compared to CH_2Cl_2. Tricoordination (e.g., as undoubtedly occurs in CH_2Cl_2 and as found in solid-state structures of **1b**,[2d] **1c**,[2a] and **1e**[4]) would tend to make the copper complex redox potentials very positive since this coordination number is essentially unknown for Cu(II);[53] an added DMF ligand generated four-coordinate Cu(I) complexes, facilitating oxidation and lowering the $E_{1/2}$ values.

In an attempt to probe the redox chemistry of the copper(II)-coordinated peroxo group in complexes $[Cu_2(Nn)(O_2)]^{2+}$ (**2**), we carried out low-temperature CV experiments, as shown in Figure 8 for $[Cu_2(N3)(O_2)]^{2+}$ (**2a**). Figure 8a shows a typical CV for precursor complex $[Cu_2(N3)]^{2+}$ (**1a**) in dichloromethane at room temperature, where one sees a reasonably well-behaved process similar to that observed in DMF. At −80 °C, the behavior for the same solution is poorer (Figure 8b), and while indicative of quasireversible behavior, the ΔE_p value of 1160 mV suggests the presence of a considerable complex and/or solvent reorganizational barrier.[52a,b] $[Cu_2(N3)(O_2)]^{2+}$ (**2a**) was formed by oxygenation of the −80 °C solution followed by Ar-bubbling for 40 min to remove excess O_2. For complex **1a** and the others only a single irreversible diffusion-controlled reduction wave was detected (Figure 8c), determined to be a one-electron process by comparison with the peak current function value of a mononuclear standard complex. No oxidative peaks in CV spectra were seen up to at least +2.0 V vs Ag/AgCl; thus, there is no evidence for the existence of a stable one-electron-oxidized species (e.g. superoxodicopper(II)?). This behavior is also consistent with our failure to isolate any species resulting from the stoichiometric chemical oxidations of complexes $[Cu_2(Nn)(O_2)]^{2+}$ (**2**) using ferrocenium ion or other one-electron oxidants. Relatively few electrochemical studies have been carried out on peroxometal complexes.[35a] *μ*-Peroxo–dicobalt(III) complexes are very difficult to oxidize,[54] and peroxo–titanium and rhodium porphyrin complexes tend to show ligand-based redox processes as well as O–O cleavage reactions to give oxo–metal species.[55] Recent cyclic voltammetric studies[56] of O_2–diiron species also indicate the occurrence of both irreversible reductive electrochemistry, and in one case it is reported that oxidation of $(DPA)_2Fe(O)(HOOH)Fe(PA)_2$ (DPA = 2,6-pyridinedicarboxylate; +1.00 V vs SCE in DMF) results in the liberation of singlet oxygen.[56b]

$[Cu_2(Nn)(O_2)]^{2+}$ (2). Additional Comparisons with Other Synthetic $\{Cu_2–O_2\}$ Complexes and Hemocyanin. While there are a number of other $\{Cu_2–O_2\}$ complexes reported in the literature,[36,57–59] comparisons with $[Cu_2(Nn)(O_2)]^{2+}$ (**2**) are most easily made with others from our own laboratories, since these all contain pyridine-amine ligand donors very similar to the PY2 moiety found in N*n* or XYL-X. We have thus far described three classes of peroxodicopper(II) complexes containing pyridine-type ligands (PY = 2-pyridyl)[1a] and more recently simple unidentate imidazole donors have been successfully employed in $\{Cu_2–O_2\}$ formation.[1c] $[Cu_2(XYL\text{-}O\text{-})(O_2)]^+$ contains an unsymmetrically bound peroxo ligand ($\nu_{O–O}$ = 803 cm^{-1}) in a phenoxo-bridged dicopper(II) unit.[11b,59] $[\{(tmpa)Cu\}_2(O_2)]^{2+}$ forms by addition of O_2 to the monomeric precursor $[(tmpa)Cu^I(RCN)]^+$, and the X-ray crystal structure reveals a trans *μ*-1,2-peroxo ligand ($\nu_{O–O}$ = 834 cm^{-1})[39b]

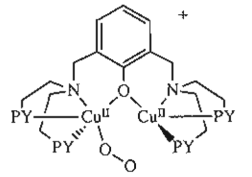

$[Cu_2{}^{II}(XYL\text{-}O\text{-})(O_2)]^+$

Terminal Peroxo Coordination

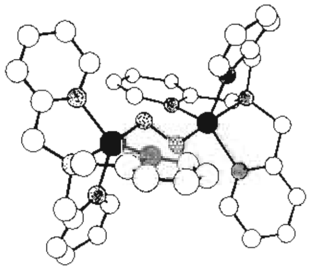

$[\{Cu^{II}(tmpa)\}_2(O_2)]^{2+}$

Trans μ-1,2-Peroxo Coordination

---

(51) Sorrell, T. N.; Malachowski, M. R.; Jameson, D. I. *Inorg. Chem.* **1982**, *21*, 3250–3252.

(52) (a) Bond, A. M.; Haga, M.; Creece, I. S.; Robson, R.; Wilson, J. C. *Inorg. Chem.* **1988**, *27*, 712–721. (b) Gennett, T.; Milner, D. F.; Weaver, M. J. *J. Phys. Chem.* **1985**, *89*, 2787–2794. (c) Drago, R. S.; Desmond, M. J.; Corden, B. B.; Miller, K. A. *J. Am. Chem. Soc.* **1983**, *105*, 2287–2296. (d) Gritzner, G.; Danksagmuller, K.; Gutmann, V. *J. Electroanal. Chem. Interfacial Electrochem.* **1976**, *72*, 177.

(53) Hathaway, B. J. In *Comprehensive Coordination Chemistry*; Wilkinson, G., Ed.; Pergamon Press: New York, 1987; Chapter 53, Vol. 5, pp 533–774.

(54) (a) Richens, D. T.; Sykes, A. G. *J. Chem. Soc., Dalton Trans.* **1982**, 1621–1624. (b) Fallab, S.; Mitchell, P. R. *Adv. Inorg. Bioinorg. Mech.* **1984**, *3*, 311–377. (c) Harris, W. R.; McLendon, G. L.; Martell, A. E.; Bess, R. C.; Mason, M. *Inorg. Chem.* **1980**, *19*, 21–26.

(55) (a) Malinski, T.; Chang, D.; Latour, J.-M.; Marchon, J.-C.; Gross, M.; Giraudeau, A.; Kadish, K. M. *Inorg. Chem.* **1984**, *23*, 3847–3955. (b) Anderson, J. E.; Yao, C.-L.; Kadish, K. M. *Inorg. Chem.* **1986**, *25*, 3224–3228.

(56) (a) Sawyer, D. T.; McDowell, M. S.; Spencer, L.; Tsang, P. K. S. *Inorg. Chem.* **1989**, *28*, 1166–1170. (b) Cofré, P.; Richert, S. A.; Sobkowiak, A.; Saywer, D. T. *Inorg. Chem.* **1990**, *29*, 2645–2651.

(57) For recent reviews of synthetic $\{Cu_2–O_2\}$ models, see: (a) Sorrell, T. N. *Tetrahedron* **1989**, *45*, 3–68. (b) Karlin, K. D.; Gultneh, Y. *Prog. Inorg. Chem.* **1987**, *35*, 219–327.

(58) A very recent report details the quasi-reversible dioxygen binding of $[Cu_2(tpmc)]^{2+}$ (tpmc = 1,4,8,11-tetrakis(2′-pyridylmethyl)-1,2,8,11-tetraazacyclotetradecane), where resonance Raman derived $\nu_{O–O}$ values of 820 and 771 cm^{-1} were also observed: Asato, E.; Hashimoto, S.; Matsumoto, N.; Kida, S. *J. Chem. Soc., Dalton Trans.* **1990**, 1741–1746.

(59) Sorrell and co-workers recently reported that peroxo and hydroperoxo complexes also form upon oxygenation of a very similar ligand dicopper complex utilizing pyrazole rather than pyridine donors: Sorrell, T. N.; Vankai, V. A. *Inorg. Chem.* **1990**, *29*, 1687–1692.

bound to trigonal-bipyramidally coordinated Cu(II) moieties.[11a] As described above, $[Cu_2(L)(O_2)]^{2+}$ (**2**) compounds are proposed to have a μ-η^2:η^2-peroxo butterfly structure. The UV-vis spectral and other physical properties of all these complexes and hemocyanin are given in Table IV.

All of these $\{Cu_2-O_2\}$ species are derived from structurally characterized copper(I) precursor complexes, by the addition of O_2 at −80 °C in dichloromethane (and/or EtCN in the case of $[(tmpa)Cu^I(RCN)]^+$). We have thus far been unable to stabilize these species at significantly higher temperatures. All three classes of complexes satisfy the criteria for identifying authentic O_2 complexes. The stoichiometry of binding of O_2 is strictly Cu:O_2 = 2:1, and an ν_{O-O} stretch consistent with the presence of peroxide (i.e. O–O bond intact) has been obtained by resonance Raman spectroscopy for two of the three classes (Table IV).[39] In all cases, O_2 is recovered by the application of a vacuum or by displacement with CO or triphenylphosphine,[60] and the O_2 released was quantified. The $\{Cu_2-O_2\}$ complexes are all characterized by strong UV–vis CT absorptions, and the reversibility of both O_2 and CO binding has been demonstrated through spectrophotometrically monitored vacuum-cycling and carbonyl-cycling experiments.

The UV–vis spectra (Table IV) of $[Cu_2(XYL\text{-}O\text{-})(O_2)]^+$ and $[\{(tmpa)Cu\}_2(O_2)]^{2+}$ show patterns that are considerably different from those of $[Cu_2(L)(O_2)]^{2+}$ (**2**). Only two CT bands are exhibited by $[Cu_2(XYL\text{-}O\text{-})(O_2)]^+$, a spectrum consistent with either terminally bound O_2 or unsymmetrically bridging peroxo coordination.[39a] The UV–vis spectroscopic features of $[Cu_2(L)(O_2)]^{2+}$ (**2**) are similar to those of oxy-Hc (vide supra), while the $[Cu(HB(3,5\text{-}iPr_2pz)_3]_2(O_2)$ complex reported by Kitajima[36] with its μ-η^2:η^2 structure (as also proposed for **2**) appears to possess very closely matching spectral features. Complete spectroscopic analyses of both **2** and $[Cu(HB(3,5\text{-}iPr_2pz)_3]_2(O_2)$ are needed before firm conclusions can be reached. The complete characterization of well-defined complexes such as $[\{(tmpa)Cu\}_2(O_2)]^{2+}$ and $[Cu(HB(3,5\text{-}iPr_2pz)_3]_2(O_2)$ is very important in obtaining a fundamental understanding of the bonding and electronic structure in Cu–O_2 complexes and developing meaningful correlations between structure and spectral (e.g., electronic and vibrational) properties.[37,39]

The elucidation of reactivity patterns as a function of $\{Cu_2-O_2\}$ structural type is also of interest. For example, $[Cu_2(L)(O_2)]^{2+}$ (**2**) reacts rather differently than do the other two types.[61] $[Cu_2(XYL\text{-}O\text{-})(O_2)]^+$ and $[\{(tmpa)Cu\}_2(O_2)]^{2+}$ react with H^+ to form hydroperoxo species, with PPh_3 liberating O_2, and with CO_2 to form percarbonates. By contrast, $[Cu_2(N4)(O_2)]^{2+}$ (**2c**) is unreactive toward stoichiometric quantities of protic acids and CO_2, it oxygenates PPh_3,[2a] and the peroxo intermediate of the related $[Cu_2(XYL\text{-}X)(O_2)]^{2+}$ hydroxylates an unactivated arene which is part of the dinucleating ligand.[1] Thus, it appears that the μ-η^2:η^2-peroxo group in complexes **2** is nonbasic and acts as an electrophilic peroxide, in contrast to the basic or nucleophilic behavior of the peroxo group in the other systems.[61] The reason for the difference in reactivity of the peroxo group in these dicopper(II) complexes is not completely clear, but presumably the difference in ligand donor sets for Cu(II) and/or the structure is important. An obvious difference between $[Cu_2(L)(O_2)]^{2+}$ (**2**) and the others is that in **2** there are only three donors per copper ion, perhaps rendering the peroxo oxygen atoms electron deficient. Ross and Solomon report that a μ-η^2:η^2-peroxo group possesses less negative charge than does a cis-μ-1,2-peroxo-coordinated O_2^{2-} group, due to a stronger π^*_σ donor interaction.[37] These observations also indirectly suggest that the unusual peroxo moiety in **2** may be closely related to that in hemocyanin and the monooxygenase tyrosinase, both of which are known to have similar active site oxy structures.[8a]

Conclusions

By employing low-temperature synthetic and spectroscopic methods, it is possible to characterize a variety of types of $\{Cu_2-O_2\}$ complexes in which the binding of dioxygen to Cu(I) precursors is reversible. The species formed from hydrocarbon-linked PY2 tridentate units L are best described as peroxodicopper(II) compounds $[Cu_2(L)(O_2)]^{2+}$ (**2**), and they provide a particularly interesting set of copper–dioxygen complexes with unusual UV–vis spectroscopic features and novel reactivity which is more typical of early transition metal peroxide compounds. Their X-ray absorption properties led us to propose that they possess a bent butterfly μ-η^2:η^2-peroxo moiety,[1a,2] a structure whose existence in the planar form has been confirmed by Kitajima and coworkers.[36]

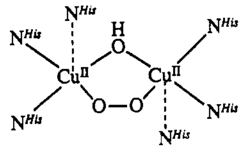

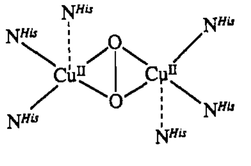

Most of the impetus for research in this area has arisen from the desire to understand (and hopefully mimic) the coordination chemistry at the active sites of proteins containing dicopper centers, e.g., hemocyanin and tyrosinase. Thus, two models for the O_2-binding structure at the active site of hemocyanin are currently being considered.[37] The one with the end-on cis-μ-1,2-peroxo and "endogenous" bridging hydroxide ligand was elaborated by Solomon and co-workers from studies on oxy-Hc and the met azide hemocyanin derivative.[6a–c] Our more recent investigations on $\{Cu_2-O_2\}$ complexes $[Cu_2(L)(O_2)]^{2+}$ (**2**), Kitajima's $Cu(HB(3,5\text{-}iPr_2pz)_3]_2(O_2)$ complex,[36] and the recent theoretical study of Ross and Solomon[37] suggest that the side-on μ-η^2:η^2 peroxo structure without any additional bridging ligand must be seriously considered. While each proposed structure has features which help explain aspects of the known protein and synthetic model chemistry, the μ-η^2:η^2-peroxo structure has attributes which cause us to favor its likelihood in the protein: (a) the electronic spectra of **2** and Kitajima's complex qualitatively resemble the LMCT spectra seen in oxy-Hc, (b) the low ν_{O-O} stretching frequency seen in oxy-Hc and Kitajima's complex is explained by this side-on peroxo structure, (c) the diamagnetism of these model complexes suggests that an endogenous hydroxide ligand is not necessary to account for the strong magnetic coupling in oxy-Hc,[36,38] and (d) the reactivity patterns seen for $[Cu_2(L)(O_2)]^{2+}$ (**2**) indicate that the peroxo unit in these compounds is capable of mediating reactions known for tyrosinase, i.e. the electrophilic attack of an arene resulting in its hydroxylation. Further spectroscopic investigations may distinguish between these two structures;[37] a high-resolution protein X-ray structure on oxyhemocyanin would be very desirable.

There is still a great deal to learn concerning copper/dioxygen structure, spectroscopy, and reactivity. For $[Cu_2(L)(O_2)]^{2+}$ (**2**), points of interest include (i) the determination of how these properties are influenced by subtle changes in L and how ligand or complex modification may stabilize and/or flatten the Cu_2O_2 core, (ii) consideration of how to make use of the electrophilic peroxide present, so as to oxygenate externally added substrates, and (iii) investigations of the kinetics and thermodynamics of O_2 binding to $Cu(I)_n$ in these systems and mechanisms of decomposition processes. Related avenues which we wish to explore involve comparisons of O_2 binding using dinuclear complexes versus complete O_2-reduction processes mediated by multinuclear copper ion centers.[62,63] We are also interested in the elucidation of the Cu^I/O_2 chemistry and design of models for other mono-

---

(60) The importance of recovering and identifying O_2 bound to copper ion has been recently emphasized in a case where the reaction of a Cu(I) complex with dioxygen (Cu:O_2 stoichiometry of 2:1) appeared to be reversible as seen by spectroscopic cycling; however, dioxygen could not be recovered from the putative $\{Cu_2-O_2\}$ adduct. See: Goodwin, J. A.; Bodager, G. A.; Wilson, L. J.; Stanbury, D. M.; Scheidt, W. R. *Inorg. Chem.* **1989**, *28*, 35–42.

(61) Paul, P. P.; Tyeklár, Z.; Jacobson, R. R.; Karlin, K. D. *J. Am. Chem. Soc.* **1991**, *113*, 5322–5332.

(62) Karlin, K. D.; Gan, Q.-F.; Farooq, A.; Liu, S.; Zubieta, J. *Inorg. Chem.* **1990**, *29*, 2249–2251.

(63) Nasir, M. S.; Karlin, K. D.; McGowty, D.; Zubieta, J. *J. Am. Chem. Soc.* **1991**, *113*, 698–700.

oxygenases, e.g. pterin-dependent copper phenylalanine hydroxylase and dopamine β-hydroxylase, which appear to utilize mononuclear copper centers in activation of O_2 by copper ions.

Acknowledgment. We are very grateful the National Institutes of Health (K.D.K., Grants GM 28962 and GM34909) for their support of this research.

Supplementary Material Available: A full table of crystal data (Table VI) and listings of bond lengths (Table VIII), bond angles (Table IX), anisotropic temperature factors (Table X), and hydrogen coordinates and temperature factors (Table XI) for **4a**$(ClO_4)_2$ and figures showing UV-vis spectra, vacuum cycling, and carbonyl cycling (11 pages); a listing of observed and calculated structure factors (Table VII) (32 pages). Ordering information is given on any current masthead page.

Contribution from the Lehrstuhl für Anorganische Chemie I, Ruhr-Universität, D-4630 Bochum, Germany,
Institut für Anorganische und Analytische Chemie der Universität, D-7800 Freiburg, Germany,
and Anorganisch-Chemisches Institut der Universität, D-6900 Heidelberg, Germany

Mono- and Dinuclear Zinc(II) Complexes of Biological Relevance. Crystal Structures of $[L_2Zn](PF_6)_2$, $[L'Zn(O_2CPh)_2(H_2O)]$, $[L'_2Zn_2(\mu\text{-}OH)_2](ClO_4)_2$, and $[L'_2Zn_2(\mu\text{-}OH)(\mu\text{-}CH_3CO_2)_2](ClO_4)\cdot H_2O$ (L = 1,4,7-Triazacyclononane, L′ = 1,4,7-Trimethyl-1,4,7-triazacyclononane)

Phalguni Chaudhuri,[1a] Claudia Stockheim,[1a] Karl Wieghardt,*[,1a] Werner Deck,[1b] Ralf Gregorzik,[1b] Heinrich Vahrenkamp,*[,1b] Bernhard Nuber,[1c] and Johannes Weiss†[,1c]

Received September 5, 1991

The macrocycle 1,4,7-triazacyclononane ($C_6H_{15}N_3$; L) reacts with Zn(II) ions in methanolic solution forming the 2:1 species $[L_2Zn]^{2+}$. The crystal structure of $[L_2Zn](PF_6)_2$ (**1**) has been determined. Crystal data: space group $C2/c$, $a = 9.719$ (2) Å, $b = 16.312$ (3) Å, $c = 15.017$ (3) Å, $\beta = 92.04$ (3)°, $V = 2379.3$ (8) Å^3, and $Z = 4$. The zinc ions are in a distorted octahedral environment of six amine nitrogen donor atoms. In contrast, the sterically more demanding tridentate macrocycle 1,4,7-trimethyl-1,4,7-triazacyclononane ($C_9H_{21}N_3$; L′) forms 1:1 species containing the L′Zn fragment. In the presence of sodium benzoate the mononuclear species $[L'Zn(O_2CPh)_2(H_2O)]$ (**2**) is generated. Crystal data: space group $P\bar{1}$, $a = 8.193$ (2) Å, $b = 12.173$ (2) Å, $c = 13.387$ (3) Å, $\alpha = 79.53$ (3)°, $\beta = 72.48$ (3)°, $\gamma = 70.93$ (3)°, $V = 1198.2$ (4) Å^3, and $Z = 2$. The Zn(II) ions are in a distorted octahedral environment composed of three facially coordinated amine nitrogen, two carboxylate oxygen atoms, and a water molecule. The two carbonyl oxygen atoms of the carboxylato groups are intramolecularly hydrogen bonded to the coordinated water molecule. In aqueous solution in the absence of coordinating ligands the L′Zn fragment was found to generate the di-μ-hydroxo-bridged dinuclear species $[L'_2Zn_2(\mu\text{-}OH)_2](ClO_4)_2$ (**3**). Crystal data: space group $P2_1/n$, $a = 8.703$ (2) Å, $b = 8.325$ (2) Å, $c = 20.470$ (4) Å, $\beta = 90.96$ (3)°, $V = 1482.9$ (6) Å^3, and $Z = 2$. The Zn(II) ions are in a distorted square base pyramidal environment (five-coordinate). In the presence of excess sodium acetate L′Zn fragments form the dinuclear species $[L'_2Zn_2(\mu\text{-}OH)(\mu\text{-}O_2CCH_3)_2](ClO_4)\cdot H_2O$ (**4**). Crystal data: space group $P4_12_12$, $a = 10.90$ (1) Å, $c = 27.86$ (1) Å, $V = 3310.0$ (10) Å^3, and $Z = 4$. The dinuclear cation contains the (μ-hydroxo)bis(μ-acetato)dizinc(II) core and two tridentate macrocyclic capping ligands. Both zinc ions are in an octahedral ligand environment. Complexes **3** and **4** serve as structural models for the spatial arrangement of the two zinc(II) ions in the active sites of the enzymes phospholipase C from *Bacillus Cereus* and leucine aminopeptidase from bovine lens, respectively.

Introduction

The synthesis and structural characterization of classical Werner-type coordination compounds of zinc(II) with N- and O-donor ligands has in the past few years experienced a dramatic resurgence.[2] This is undoubtedly triggered by the rapidly growing knowledge of the structures of zinc-containing active sites of a variety of enzymes. While the majority of these appear to contain one zinc(II) ion in their respective active site,[3] there have recently been reported the structures of two enzymes which contain two zinc ions in close proximity (<3.4 Å) in the respective active site.[4,5] In the enzyme phospholipase C from *Bacillus cereus* there are three zinc(II) ions per subunit, two of which are at a distance of 3.3 Å. These two are connected by one symmetrical carboxylate bridge (Asp 122) and a bridging OH^- or H_2O group. All three metal ions are approximately trigonal bipyramidal. The ligand environment of the dinuclear part is shown schematically in Chart Ia. In contrast, bovine lens leucine aminopeptidase contains two zinc(II) ions at a distance of only 2.88 Å. Since the structure of this enzyme has been refined at 2.7 Å resolution, the exact nature of the first coordination spheres around the zinc ions has not been fully established. A sketch is shown in Chart Ib. Most importantly from our perspective, no single atom bridging groups H_2O or OH^- have been identified which could account for the rather short Zn⋯Zn distance. Aspartate-255 and glutamate-334 are suggested to form two carboxylate bridges. It is our aim to provide circumstantial evidence from low-molecular-weight model complexes how the two zinc ions can be forced at this close distance.

Chart I

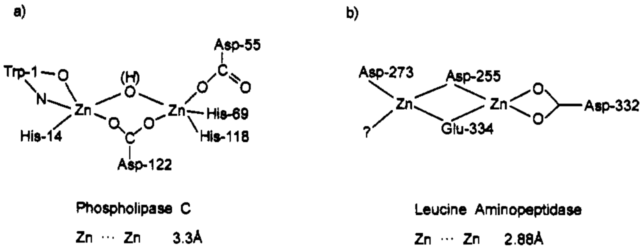

Phospholipase C
Zn ⋯ Zn 3.3Å

Leucine Aminopeptidase
Zn ⋯ Zn 2.88Å

Lacking ligand field stabilization energy, zinc(II) exhibits no preferential, electronically favored coordination number, and consequently, four-, five-, and six-coordinate complexes are most

---

† Deceased.

(1) (a) Ruhr-Universität Bochum. (b) Universität Freiburg. (c) Universität Heidelberg.

(2) Prince, R. H. In *Comprehensive Coordination Chemistry*; Wilkinson, G., Gillard, R. D., McCleverty, J. A., Eds.; Pergamon Press: Oxford, England, 1987; Vol. 5, p 925.

(3) (a) Spiro, T. G., Ed. *Zinc Enzymes*; Wiley: New York, 1983. (b) Sigel, H., Ed. *Zinc and its Role in Biology and Nutrition*; Marcel Dekker: New York, 1983. (c) Erkisson, E. A.; Jones, T. A.; Liljas, A. In *Zinc Enzymes*; Birkhäuser: Boston, MA, 1986.

(4) Hough, E.; Hansen, L. K.; Birknes, B.; Jynge, K.; Hansen, S.; Hardvik, A.; Little, C.; Dodson, E.; Derewenda, Z. *Nature* **1989**, *338*, 357.

(5) Burley, S. K.; David, P. R.; Taylor, A.; Lipscomb, W. N. *Proc. Natl. Acad. Sci. U.S.A.* **1990**, *87*, 6878.

0020-1669/92/1331-1451$03.00/0